Spacecraft Design-for-Demise Strategy, Analysis and Impact on Low Earth Orbit Space Missions

by

Waswa M.B. Peter

M.Sc., Space Studies
International Space University, 2005

B.Sc., Electrical & Electronics
Jomo Kenyatta University of Agriculture and Technology, 2000

Submitted to the Department of Aeronautics and Astronautics
in Partial Fulfillment of the Requirements for the Degree of
Master of Science in Aeronautics and Astronautics

at the

MASSACHUSETTS INSTITUTE OF TECHNOLOGY

February 2009

Signature of Author:.....

Department of Aeronautics and Astronautics
January 26, 2009

Certified by:.....

Dr. Jeffrey A. Hoffman
Professor of the Practice of Aerospace Engineering
Thesis Supervisor

Accepted by:.....

Prof. David L. Darmofal
Associate Department Head
Chair, Committee on Graduate Students

(This page is intentionally left blank)

Spacecraft Design-for-Demise Strategy, Analysis and Impact on Low Earth Orbit Space Missions

by

Waswa M.B. Peter

Submitted to the Department of Aeronautics and Astronautics
on January 26, 2009 in Partial Fulfillment of the
Requirements for the Degree of
Master of Science in Aeronautics and Astronautics

Abstract

Uncontrolled reentry into the Earth atmosphere by LEO space missions whilst complying with stipulated NASA Earth atmospheric reentry requirements is a vital endeavor for the space community to pursue. An uncontrolled reentry mission that completely ablates does not require a provision for integrated controlled reentry capability. Consequently, not only will such a mission design be relatively simpler and cheaper, but also mission unavailability risk due to a controlled reentry subsystem failure is eliminated, which improves mission on-orbit reliability and robustness.

Intentionally re-designing the mission such that the spacecraft components ablate (demise) during uncontrolled reentry post-mission disposal is referred to as Design-for-Demise (DfD). Re-designing spacecraft parts to demise guarantees adherence to NASA reentry requirements that dictate the risk of human casualty anywhere on Earth due to a reentering debris with $KE \geq 15J$ be less than 1:10,000 (0.0001). NASA sanctioned missions have traditionally addressed this requirement by integrating a controlled reentry provision. However, momentum is building for a new paradigm shift towards designing reentry missions to demise instead.

Therefore, this thesis proposes a DfD decision making methodology; DfD implementation and execution strategy throughout the LEO mission life-cycle; scrutinizes reentry analysis software tools and uses NASA Debris Analysis Software (DAS) to demonstrate the reentry demisability analysis process; proposes methods to identify and redesign hardware parts for demise; and finally considers the HETE-2 mission as a DfD demisability case study. Reentry analysis show HETE-2 mission to be compliant with NASA uncontrolled atmospheric reentry requirements.

Thesis Supervisor: Jeffrey A. Hoffman
Title: Professor of the Practice of Aerospace Engineering

(This page is intentionally left blank)

Acknowledgments

I would like to express my deepest gratitude to Professor Jeffrey A. Hoffman for his guidance, encouragement and support as my academic and thesis advisor. His dedication contributed immensely towards timely completion of this thesis. I am also grateful to Professor George E. Apostolakis for providing funding for this investigation and Michael Stawicki for his tireless reviews and input especially on the Analytic Decision Process.

Dr. N. Johnson and J. Opiela of the Orbital Debris Program Office (NASA Lyndon B. Johnson Space Center, Houston, Texas) provided valuable deeper insight into NASA reentry practices and DAS dynamic aerothermal modules behavior. The office also frequently conducted further reentry analysis in ORSAT on our behalf; I am indeed sincerely appreciative of their assistance. Thank you Dr. Joel Villasenor of MIT Kavli Institute for Astrophysics and Space Research for the HETE-2 data and sample hardware parts you willingly provided.

May I also express gratitude to Professor Hugh Hill of International Space University for his guidance, encouragement and belief in me reaching my goals. Last but not least, I am deeply grateful to my parents for their selfless dedication to me since birth. They made me the person I am today, and even though we rarely see each other, I am always in their prayers.

In Loving memory of my beloved grandparents, H. Nyamwatta and J. Ekonya

Contents

Nomenclature

ADC	Attitude Determination & Control
ADP	Analytic Deliberative Decision-Making Process
AHP	Analytic Hierarchy Process
AIM	Aeronomy of Ice in the Mesosphere
C& DH	Command & Data Handling
CDR	Critical Design Review
CESR	Centre d'Etude Spatiale des Rayonnements
CGRO	Compton Gamma Ray Observatory
CNES	Centre Nationale d'Etudes Spatiales
CNR	Consiglio Nazionale delle Ricerche
COPV	Composite Overwrapped Pressure Vessels
DART	Demonstration for Autonomous Rendezvous Technology
DAS	Debris Assessment Software
DCA	Debris Casualty Area
DfD	Design-for-Demise
DPR	Dual Frequency Precipitation Radar
DR	Decommissioning Review
ESA	European Space Agency
GEO	Geosynchronous Orbit
GLAST	Gamma-ray Large Area Space Telescope
GNC	Guidance Navigation & Control
GPM	Global Precipitation Measurement
HST	Hubble Space Telescope
HETE	High Energy Transient Explorer
IAPC	Inter Agency Propulsion Committee
INPE	Instituto Nacional de Pesquisas Espaciais
ISS	International Space Station
JANNAF	Joint Army, Navy, NASA, Air Force
KDP	Key Decision Point
KE	Kinetic Energy
LANL	Los Alamos National Laboratory
LEO	Low Earth Orbit

MCR	Mission Concept Review
MDR	Mission Definition Review
MEO	Middle Earth Orbit
MKI	Kavli Institute for Astrophysics and Space Research
NACA	National Advisory Committee for Aeronautics
NASA	National Aeronautics and Space Administration
NPR	NASA Procedural Requirement
ORSAT	Object Reentry Survival Analysis Tool
PDR	Preliminary Design Review
PE	Potential Energy
PMW	Passive Microwave
PRR	Production Readiness Review
RDT&E	Research Development Testing & Evaluation
RIKEN	Institute for Chemistry and Physics
RPM	Revolutions Per Minute
RWA	Reaction Wheel Assembly
SCARAB	Spacecraft Atmospheric Re-entry and Aero-thermal Breakup
SESAM	Spacecraft Entry Survival Analysis Module
SIR	System Integration Review
SRR	System Requirements Review
Sup'Aero	Ecole Nationale Superieure de l'Aeronautique et de l'Espace
TIFR	Tata Institute of Fundamental Research
TRL	Technology Readiness Review
TT&C	Telemetry Tracking & Control
VHF	Very High Frequency

List of Figures

List of Tables

(This page is intentionally left blank)

Chapter 1

Introduction

1.1 Purpose

This thesis investigates the intentional design of space missions passing through Low Earth Orbit (LEO) while in operation, such that, upon uncontrolled reentry into the Earth's atmosphere, the spacecraft is completely ablated (demised). LEO refers to orbits below 2,000 km above the Earth surface. Spacecraft atmospheric reentry is normally initiated during post-mission disposal phase; however, reentry is not necessarily restricted to this phase of the mission. Compelling reasons such as critical system failures may lead to premature mission conclusion forcing early controlled atmospheric reentry. This thesis further investigates demisable mission implementation strategy and impact of Design-for-Demise (DfD) on the various aspects of the mission, such as mission design, reliability, availability, and performance among others. In order to explicitly distinguish demisable LEO space missions, this thesis will also classify demisable space missions in general according to their functional objectives. The key findings realized are intended to spur the view and approach to DfD in Earth atmospheric reentry mission designed by NASA and the space community at large.

1.2 Background Information

Impetus for Design-for-Demise is drawn from the requirement to guarantee safety on the ground due to reentering spacecraft debris. Intentional Atmospheric reentry of LEO spacecraft is a relatively lower cost and effective method of orbital debris mitigation through

non-contribution of new debris into orbit. DfD facilitates ablation of spacecraft parts during the dynamic reentry process thereby guaranteeing ground safety. Moreover, since DfD eliminates the provision for controlled reentry on the spacecraft; it relatively simplifies the space mission, lowers cost and risk while meeting the NASA requirements for limiting creation of new orbital debris.

Design of NASA missions reentering Earth's atmosphere must comply with *Requirement 4.7-1* of the the NASA Technical Standard 8719.14 - *Process for Limiting Orbital Debris* outlined below[1]:

> *Requirement 4.7-1. Limit the risk of human casualty*: The potential for human casualty is assumed for any object with an impacting kinetic energy in excess of 15 Joules:
> a) For uncontrolled reentry, the risk of human casualty from surviving debris shall not exceed 0.0001 (1:10,000) (Requirement 56626).

Before we proceed, let us define uncontrolled reentry and human casualty risk.

Uncontrolled Reentry: The atmospheric reentry of a space structure where the subsequent surviving debris cannot be guaranteed to avoid landing on a landmass.

Human Casualty Risk: The chance of a human casualty occurring on Earth due to space debris. According to the 1995 NASA policy (endorsed in 2001 by the U.S. Government Orbital Debris Mitigation Standard Practices); the risk of world-wide human casualty from a single uncontrolled reentering space structure shall not exceed 1 in 10,000 [2].

DfD offers a relatively cheaper, effective and simplified means of meeting the aforementioned requirement for Earth reentering LEO missions. According to the US Government Orbital Debris Mitigation Standard Practices [2], missions passing through LEO with a perigee altitude below 2,000 km shall be disposed of by: *a*) atmospheric reentry through controlled de-orbit as soon as practical after mission completion; or uncontrolled natural de-orbit resulting in reentry within 25 years after mission completion but not more than 30 years after launch, *b*) maneuvered to a storage regime between LEO and Middle Earth Orbit (MEO) with perigee altitude above 2,000 km and apogee altitude of 500km below Geosynchronous Orbit (GEO) and *c*) direct retrieval of the space structure within 10 year after mission completion.

Within NASA, critical attention to DfD intensified after the Compton Gamma Ray Observatory (CGRO) mission (launched on 5 April 1991) was prematurely de-orbited on 4 June 2000 despite the observatory payload being operationally sound. The premature disposal was as a consequence of the zero fault tolerance stance adopted by NASA after one of the three gyroscopes failed. Though the observatory could have been satisfactorily oriented in space by the remaining two gyroscopes, controlled reentry would have been rendered unachievable if one more gyroscope failed. Consequently, to guarantee the safety of people on the ground, mission managers decided to safely de-orbit the spacecraft while they still had full control [3]. If the CGRO mission had been designed for demise, the unfortunate premature decommission of this spacecraft could have been avoided and opportunity for scientific study protracted.

Moving forward, after the CGRO experience, another NASA mission, Gamma-ray Large Area Space Telescope (GLAST) explored further the issue of designing for demise [4]. An illustration of GLAST spacecraft in orbit is shown in Figure 1.1. Faced with a dilemma of having to incorporate a de-orbit propulsion system though none was required for normal in-orbit payload operation, DfD outrightly presented a perfect solution. DfD would simplify the spacecraft design and lower costs. Possible modifications on the spacecraft to replace non-demisable parts with demisable ones, excluding the propulsion subsystem, were analyzed. However, a Kinetic Energy (KE) threshold for objects surviving reentry as stipulated by *Requirement 4.7-1* above had not yet been adopted by NASA. Though the reentry analysis team managed to meet the 1:10,000 human casualty risk threshold for surviving debris with a KE of less than 30 Joules, uncertainty in the KE threshold value forced the mission to maintain a controlled reentry baseline and single fault tolerant design [5]. Nevertheless, GLAST addressed the issue of Design-for-Demise deeper than any other NASA mission before it. GLAST mission was successfully launched on 11 June 2008 at 1:20 p.m. By the time of writing this thesis, GLAST is undergoing a 60 day check-out period to be followed by routine science operations. Further, NASA in collaboration with international partners is planning the the Global Precipitation Measurement (GPM) mission. In addition to a core spacecraft scheduled for launch on 21 July 2013, GPM sensor web will consist of a constellation of eight spacecraft. GPM is hence a next generation satellite-based Earth science mission that will study global precipitation namely rain, snow and ice [6]. The core spacecraft will fly both a Dual Frequency Precipitation Radar (DPR) and a high resolution,

Figure 1.1: GLAST Mission. (Courtesy: NASA Goddard Space Flight Center)

multi-channel passive microwave (PMW) rain radiometer known as the GPM Microwave Imager. GPM is intended to be the the first fully designed for demise LEO mission. The post-mission disposal objective is to meet *Requirement 4.7-1* stated above exclusively by design practices. GPM is in the formulation stages.

Evidently, NASA, United States Government and other leading global players in the space arena have subscribed to unfaltering commitments on orbital debris mitigation practices and acceptable human casualty risk from space debris. Accordingly, due to these obligations, designing spacecraft destined for uncontrolled atmospheric reentry to demise will provide a cost-effective solution to the challenge. Moreover, DfD will also introduce a post-mission disposal paradigm shift in the design of space missions passing through LEO.

1.3 Thesis Scope and Overview

As outlined in section 1.1, this thesis addresses the approach strategy to DfD, carries out analysis and investigates DfD impact on LEO space missions. Perusal of pertinent literature followed by computation of relevant data and analysis via appropriate software tools will comprise the fundamental source of the results to be obtained. This thesis is divided into chapters as summarized in Figure 1.2 to conduct this investigation.

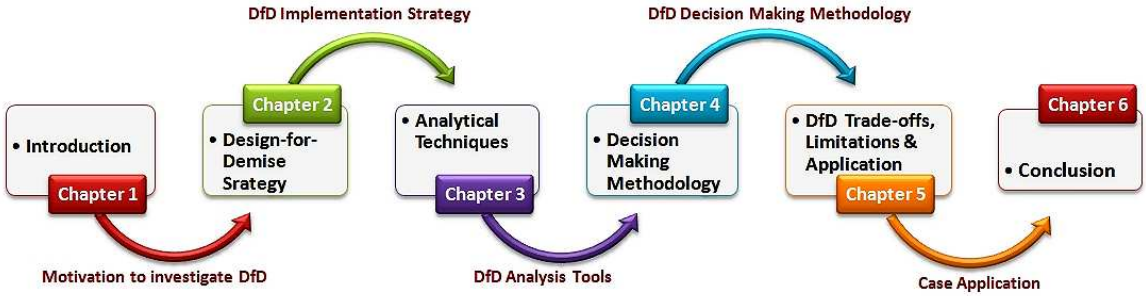

Figure 1.2: Thesis road map.

Chapter 2 formally introduces and defines what is DfD. Further, the present NASA implementation of DfD and how it affects reentry LEO mission design is scrutinized. To put into perspective the types of missions that DfD can be applied to, we categorize general demisable missions according to their purpose. Moreover, we draw a contrast between the prevailing approach to DfD by NASA and the new approach to DfD of LEO misions proposed by this thesis. The demisable LEO mission categorization emphasizes that DfD is not limited to missions with a particular type of mission objective. DfD can be employed right across the board on any type of mission.

In Chapter 3, we introduce the analytical techniques employed to deduce the atmospheric reentry behavior of different object shapes, sizes and materials. We explore the Debris Assessment Software (DAS) tool available to download from the website of NASA Orbital Debris Program Office located at the Johnson Space Center, Houston, Texas. The breadth and limits of DAS as a reentry analysis tool are examined deeper. Further, other debris survivability analysis tools are mentioned. This chapter also lays down the foundation for subsequent demisability analysis by offering a generic spacecraft subsystems hierarchical subdivision. The subsystems hierarchical subdivision facilitates identification of critical spacecraft parts via demisability reentry analysis. The mathematical models, inputs and procedure for obtaining the reentry analysis results are described in this chapter. Finally, we demonstrate typical DAS results and how to interpret them.

Chapter 4 investigates a decision making methodology that will facilitate the decision to design a mission for demise as a post-mission disposal option. This chapter also scrutinizes the elements contained in the procedure and carries out the associated computational re-

quirements necessary to facilitate the process. The proposed process should bring together the decision maker and all the stakeholders concerned to deliberate and facilitate a consesus.

Chapter 5 will examine hardware DfD methods, trade-offs, and limitations of DfD on the spacecraft. By analyzing parts from representative subsystems that perennially survive reentry we intend to show how trade-offs can be conducted in choosing demisable parts and show the limitations in designing demisable parts. This chapter will also apply the DfD analysis techniques described beforehand to a specific LEO mission and interprete the results obtained.

Lastly, Chapter 6 summarizes key findings of this investigation. This chapter also outlines the contributions made to DfD objectives, mission formulation and mission execution practices. To connclude, we identify areas that require further examination.

Chapter 2

Strategy for Design-for-Demise

To successfully execute Design-for-Demise, first, we must define DfD and the scope within which it is applied. Hence this chapter will also categorize all potential demisable space missions according to their function in order to characterize the breadth of DfD dispensation. Then, we look at NASA's past and present approach to DfD practices exercised during mission development. Finally, this chapter proposes a framework to embed DfD in development of LEO space missions.

2.1 Design-for-Demise

Design-for-Demise is the intentional design of spacecraft hardware such that the spacecraft will completely ablate (demise) upon uncontrolled atmospheric reentry during post-mission disposal. Demisability is necessary to reduce the risk of human casualty and damage to property on Earth, and guarantee safety from satellite atmospheric reentries. For NASA sanctioned missions in particular, the debris surviving atmospheric reentry must satisfy *Requirement 4.7-1* of NASA Technical Standard 8719.14 - *Process for Limiting Orbital Debris* [1]; as outlined in section 1.2. Objects reentering the atmosphere are termed demised (ablated) when they have fully melted. Objects of different shapes, sizes and material have different ablation behaviors. For instance, aluminum and copper objects tend to burn up in the atmosphere whereas beryllium, stainless steel, titanium, and nickel objects tend to survive [7]. In general, for objects with similar shapes and sizes, those with higher melting temperatures tend to survive reentry compared to objects with relatively lower melting tem-

Table 2.1: Thermo-physical properties influencing atmospheric reentry thermal loads for common aerospace materials.

Material	**Specific Heat (J/kg-K)**	**Heat of Fusion (J/kg)**	**Melt Temperature (K)**
Aluminum	1110	390,000	850
Beryllium	1675.4<Cp<3594.8	1093220	1557
Copper	389.4<Cp<471.8	204921	1356
Nickel	440<Cp<726.7	309803	1728.2
Stainless Steel	600	270000	1700
Titanium	600	470000	1950

peratures - which tend to burn up. To illustrate, in Table 2.1, the thermo-physical properties of demisable materials mentioned above are distinguished by relatively lower melting points [8]. Where the the thermal properties are defined as:

Specific Heat: The measure of heat energy needed to raise the temperature of 1 kg of the material by 1 Kelvin interval.

Heat of Fusion: The amount of heat required to convert 1 kg mass of the material at its melting point into liquid without an increase in temperature.

Melt Temperature The temperature at which the material changes state from solid to liquid.

A reentering object undergoes heating due to dissipation of initial Potential Energy (PE) and Kinetic Energy (KE) through two heat transfer mechanisms, convection and radiation. Convective heating occurs when the object's wall is bathed in a hot fluid stream by air heated via passage through a strong bow shock in front of the object. Radiative heating occurs as well if the heated air is hot enough. Consequently, the object experiences two kinds of thermals loads: *a*) total heat load and *b*) instantaneous heating . Total heat load is significant because increase in energy input will raise the average vehicle temperature. Similarly, the permitted heating rate (local or body averaged) induces a thermal gradient from heat flux according to Fourier's law [9]:

$$p = -\kappa \nabla T \tag{2.1}$$

Where:
p = power per unit area, W/m^2
κ = thermal conductivity, W/mK
∇T = gradient of temperature, K/m

The net heating of a reentering object is obtained by the sum of convective, radiative and chemical heating less the radiative cooling as given in Equation 2.2. Radiative cooling accounts for the reradiation of heat away from the hot outer surface of the object[10].

$$q_{net} = q_{conv} + q_{rad} + q_{ox} - q_{rr} \tag{2.2}$$

Where:
q_{conv} = average aerodynamic heating
q_{rad} = gas cap radiation heating
q_{ox} = oxidation heating
q_{rr} = reradiative cooling

Heat of ablation is the best indicator of a component's ability to survive reentry. Equation 2.3 obtains Heat of ablation for a given object during atmospheric reentry [11].

$$H_{Ablat} = Mass \times [C_p \times (T_{melt} - T_{init}) + H_{Fusion}] \tag{2.3}$$

Where:
C_p = specific heat, J/kg-K
T_{melt} = melt temperature, K
T_{init} = initial object temperature, K
H_{Fusion} = heat of fusion, J/K

To estimate the amount of material ablated during reentry, we need to consider the heat-absorbing effectiveness Q^* (J/kg) of a material [12] . When a solid material undergoes a phase change with hot air rushing over the surface, a considerable increase in volume occurs. A cooling film over the surface is created which is a major factor in the effectiveness of the ablation process. This can increase the phase change heat-aborbing capability of the

material. Considering the heat energy balance equation:

$$Heat\ input = heat\ absorbed$$

$$\dot{Q}_{in} = Q^* \dot{m} \tag{2.4}$$

or

$$\dot{q}A = Q^* \rho_m A \dot{b} \tag{2.5}$$

Rearranging

$$\dot{b} = \dot{q}/\rho_m Q^* \tag{2.6}$$

Where:
A = area
b = material thickness
$\dot{m}$ = mass flow rate
$\dot{q}$ = heating rate
Q = heat energy
Q^* = total heat-absorbing effectiveness
ρ_m = material density

Typically, object burn up occurs within a range of approximately 80 km to 55 km altitude. Conversely, object cooling leading to its survival occurs below 50 km altitude as described in Section 3.1.

2.2 Classification of Demisable LEO Missions

Demisable missions passing through LEO are not restricted to those of a particular objective. DfD can be applied to spacecraft of a wide range of mission purpose. Consequently, Figure 2.1 categorizes missions passing through LEO according to the nature of their function.

1. **Earth Observation Missions:** These are missions whose payload investigates given phenomena occurring on Earth. The instruments on board function across the electromagnetic spectrum, ranging from radio waves, visible light, to gamma rays. Most

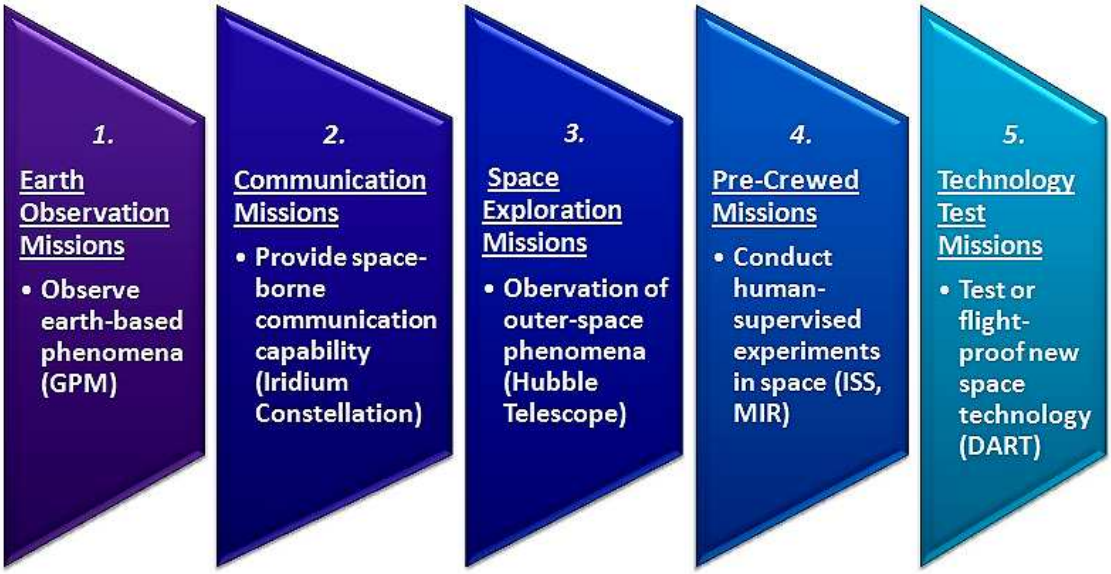

Figure 2.1: Categories of demisable LEO missions.

Earth Observation Missions are managed by government agencies and many demisable missions are likely to fall into this category. Examples of Earth Observation Missions include: GPM, AQUA, and AIM.

2. **Communication Missions:** Missions that extend communication capability on Earth whilst passing through LEO constitute this category. Their payload is primarily communication transponders and operate within a wide range of communication frequency bands depending on the application. Communication missions are managed by both government agencies and the private sector. They have a typical life span of five years, consequently, a choice of post-mission disposal by uncontrolled reentry compels them to be made demisable. Examples of communication missions include: Iridium constellation, Globalstar and Orbcomm.

3. **Space Exploration Missions:** These missions carryout scientific investigation of space phenomena. Though passing through LEO, these missions are focused on scientific scrutiny of all other phenomena in space except the Earth. Space Exploration Missions investigate phenomena like asteroids, comets, planets, stars, solar winds, and

cosmic rays among others. They are mostly managed by governmental organizations and are an excellent candidate for DfD. Examples of Space Exploration Missions include Hubble Space Telescope, GLAST, and CGRO.

4. **Pre-crewed Missions:** This category consists of abandoned space habitats that were previously manned. Such pre-crewed missions do not include crewed space vehicles initially intended to return astronauts back on Earth. Designing crewed missions that would be disposed via uncontrolled reentry is indeed a challenging task. However, this does not disqualify demisable pre-crewed missions from being implemented. Traditionally, government agencies have managed such missions, but, with the excitement within the private sector in space tourism, this is likely to change in the near future. Examples of pre-crewed missions include ISS, MIR and SKYLAB. ISS is still in orbit and though MIR and SKYLAB reentered the atmosphere, they were not demisable.

5. **Technology Test Missions:** The objective of Technology Test Missions is to flight-test new space technologies or flight-proof existing technologies that have not been flown in space. They are chiefly experimental missions that terminate once the technologies have been satisfactorily demonstrated. Consequently, the objective Technology Test Missions may even be to demonstrate desimability of given spacecraft hardware components. Different types of stake holders in the space industry like governments, agencies, universities, military and private companies manage such missions. An example is the NASA DART Mission.

From the above broad classification of demisable missions passing through LEO, the enormous potential for DfD as a factor in mission formulation and design is evident.

2.3 Current NASA Approach to DfD

Presently, Design-for-Demise of reentry NASA missions is handled within the framework of limiting orbital debris as stipulated in Procedural Requirement 8715.6A - *Limiting Orbital Debris* [13], and Technical Standard 8719.14 - *Process for Limiting Orbital Debris* [1]. However, no formal DfD requirements exist, hence, DfD is more or less implemented in an ad hoc manner. As outlined in Section 1.2, a sustained analysis of the demisability of a reentering spacecraft has only previously been undertaken on the GLAST spacecraft. Prior to the

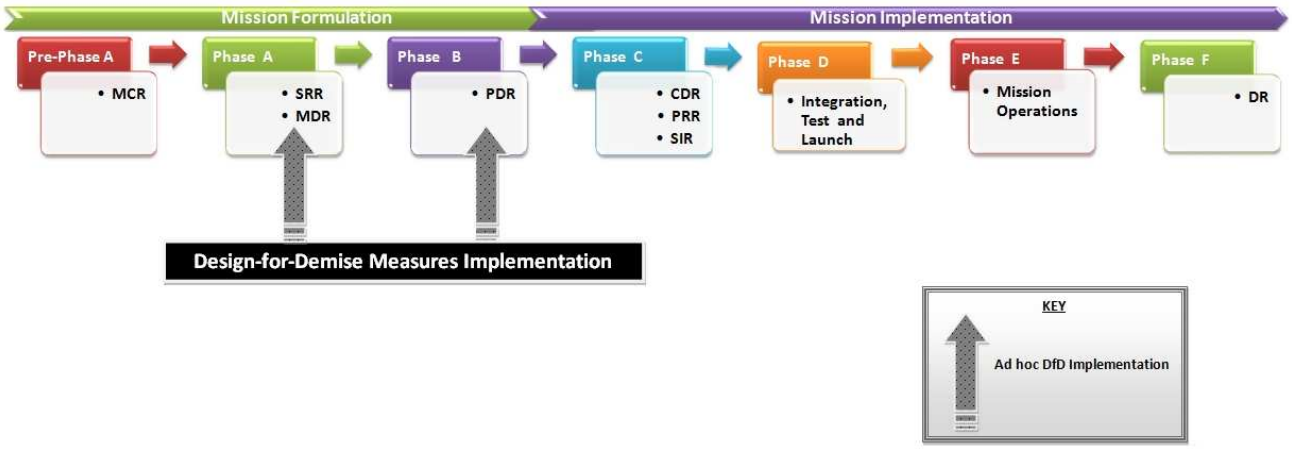

Figure 2.2: NASA Design-for-Demise implementation in reentry mission life-cycle.

Table 2.2: Key Decision Points.

CDR:	Critical Design Review	**DR**:	Decommissioning Review
MCR:	Mission Concept Review	**MDR:**	Mission Definition Review
PDR:	Preliminary Design Review	**PRR:**	Production Readiness Review
SIR:	System Integration Review	**SRR:**	System Requirements Review

GLAST mission, no consequential intentional alternative design of spacecraft hardware with the aim of making them demisable had been performed to that detail. Moreover, prior to August 2007, the more *'DfD friendly'* thresholds for Human Casualty Risk of 1:10,000 and $15J$ KE levels for objects impacting the earth were still evolving. This is evident in NASA Management Instruction 1700.8 and NASA Safety Standard 1740.14 [11], which preceded NASA directives Procedural Requirement 8715.6A [13], and Technical Standard 8719.14 [1] respectively. DfD was partially or hardly considered during reentry missions formulation phases largely because of the existence of the proven and reliable controlled reentry option.

Clearly, DfD has been loosely integrated in mission formulation by NASA. Consequently, the advantages due to DfD given in section 1.2 have often been overlooked. Moreover, the NASA DfD integration in the reentry mission life-cycle as shown in Figure 2.2 portrays the inherent weaknesses in the approach. A deeper scrutiny into the mission phases reveals the following:

- **Pre-Phase A:** (Concept Studies)
  Opportunities to identify the feasibility of mission architectures employing DfD in post-mission disposal phase are overlooked. Consequently;
  - DfD stakeholders will not be identified and engaged in the mission concepts development and trade-offs.
  - Demisability top-level system requirements are not identified.
  - NASA Technical Standard 8719.14 - *Process for Limiting Orbital Debris* [1] is not invoked at this stage to measure disposal effectiveness and compliance.
  - Preliminary demisability missions evaluation are not performed as part of the possible missions evaluation.
  - Demisability is not defined as a mission objective, hence it will not be a mission design driver.
  - DfD technology status and maturation strategies are not assessed.
- **Phase A:** (Concept and Technology Development)
  The initial baseline concept established lacks a clear approach to demisability as a post-mission disposal option hence DfD feasibility and desirability may not be exhaustively determined. Consequently;
  - Top-level Design-for-Demise requirements and constraints are not fully developed.
  - Preliminary systems requirements allocated to lower levels lack DfD requirements.
  - Demisability trade studies are not satisfactorily performed.
  - The reentry mission architecture developed at this phase excludes demisability and probably uncontrolled reentry.
  - Demisability analyses to establish compliance with *Requirement 4.7-1* of NASA Technical Standard 8719.14 [1] are absent at this stage.
  - DfD technical resource and tools are not estimated and acquired respectively.
  - Risk analysis due to DfD and subsequent appropriate risk management plans are not developed.
  - Demisability engineering specialty plans are not prepared.

  - Demisability during uncontrolled reentry is not included in the mission safety and assurance plans.
  - Technology development plans lack provisions to develop the necessary DfD technology.
  - MDR preparations partially or completely lack demisability as a post-mission disposal option.

- **Phase B:** (preliminary Design and Technology Completion)
  Design-for-Demise process will not be included in the mission preliminary design concept which details: mission top level performance requirements; and a complete set of system and subsystem design specification. Consequently:
  - Progress related to DfD technology maturity, risk analysis, mission safety and assurance will not be updated.
  - Top-level requirements finalized and flowed down to the next level lack demisability or uncontrolled reentry requirements.
  - Validation plans, design drawings, baseline specifications, and interface documents to lower levels established exclude DfD specifications.
  - Further trade studies may not wholly address demisability.
  - The favoured solution excludes demisability and uncontrolled reentry option.
  - Preliminary orbital debris and post-mission disposal analysis reports exclude spacecraft demisability analysis.
  - PDR preparations do not serve to escalate demisability and uncontrolled reentry as an option to be adopted in mission implementation for post-mission disposal.

The given mission phases are as described in the NASA Systems Engineering Handbook [14]. In the formulation phases, the major Key Decision Points (KDP) have been emphasized to show the barrier to be overcome by the design team prior to proceeding to the subsequent phase.

The flow diagram in Figure 2.3 summarizes the strategy on how DfD practices have been executed in previous NASA mission development. The *Further Formulation Phases* consist

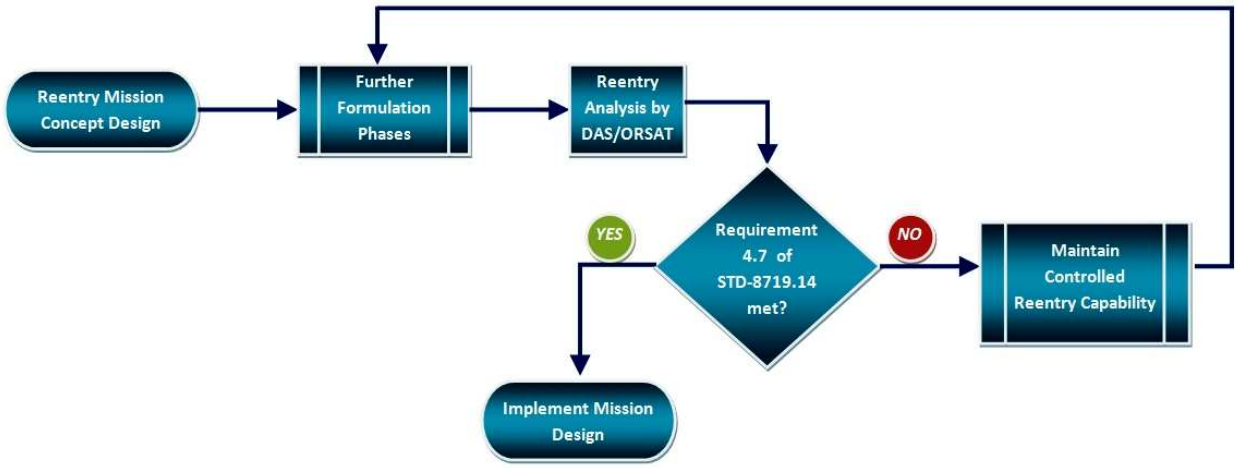

Figure 2.3: NASA Design-for-Demise execution strategy.

of **Phase A** , and **Phase B**. *Reentry Analysis* analyzes the demisability likelihood and is first performed by DAS, then further analyzed by ORSAT described in Section 3.1.

Evidently, the aforementioned approach barely qualified DfD as a mission design driver which results in lost opportunity to relatively simplify the mission and reduce costs. Ad hoc implementation of DfD practices at the later stages of mission formulation is apparent, chiefly because DfD was not entrenched as a mission design driver. Unfortunately, this approach presents significant design challenges at the later stages of mission formulation. Consequently, controlled reentry capability was automatically retained instead of exploring a 're-design' of the mission concept.

2.4 Proposed Approach to DfD

This thesis proposes accounting for Design-for-Demise as a demisable LEO mission design driver. Consequently, DfD would be entrenched and executed at all mission formulation phases. Unlike the case in section 2.3, DfD practices are present in all mission formulation phases and, of course, during the actual post-mission disposal by reentry as shown in Figure 2.4.

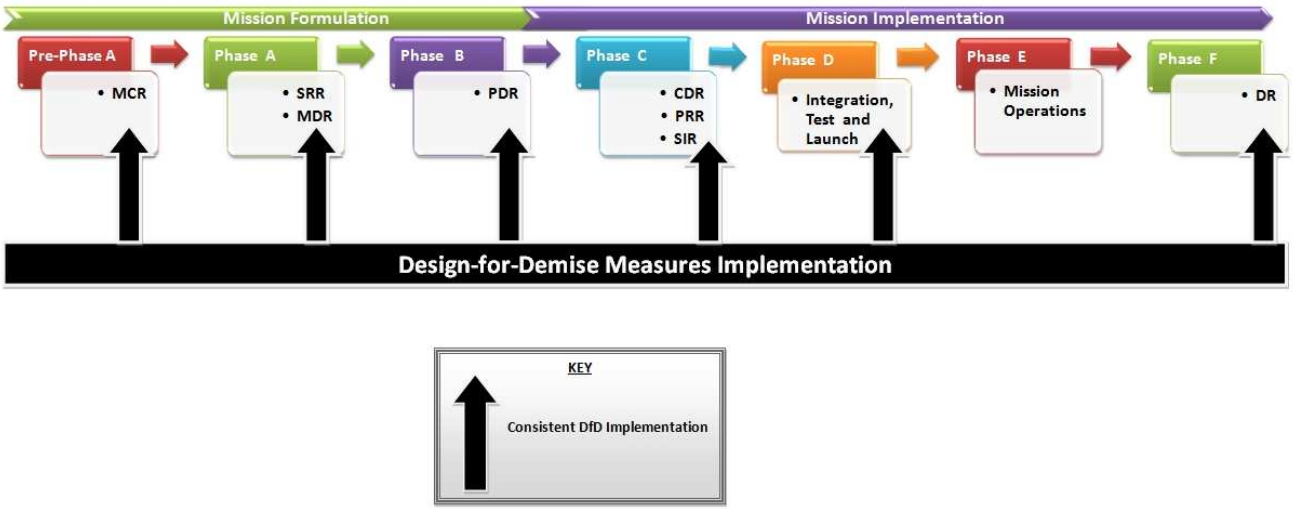

Figure 2.4: Proposed Design-for-Demise implementation in reentry mission life-cycle.

Once again, a deeper scrutiny into the mission phases reveals the following:

- **Pre-Phase A:** (Concept Studies)
  Opportunities to identify the feasibility of mission architectures employing DfD in post-mission disposal phase are exhaustively explored. Consequently:
  - DfD stakeholders are be identified and engaged in the mission concepts development and trade-offs.
  - Demisability top-level system requirements are identified.
  - NASA Technical Standard 8719.14 - *Process for Limiting Orbital Debris* [1] is invoked at this early stage to measure disposal effectiveness and requirement compliance.
  - Preliminary demisability mission evaluations are performed as part of the possible missions evaluation.
  - Demisability is defined as a mission objective and hence is entrenched as a mission design driver.
  - DfD technology status and maturation strategies are comprehensively assessed.

- **Phase A:** (Concept and Technology Development)
  The initial baseline concept established contains a clear approach to demisability as a post-mission disposal option, hence DfD feasibility and desirability are thoroughly determined. Consequently:
  - Top-level Design-for-Demise requirements and constraints are fully developed.
  - Preliminary systems requirements allocated to lower levels carry DfD requirements.
  - Demisability trade studies are satisfactorily performed.
  - The reentry mission architecture developed at this phase includes demisability and probably uncontrolled reentry option.
  - Initial demisability analysis to establish compliance with *Requirement 4.7-1* of NASA Technical Standard 8719.14 [1] are performed this stage.
  - DfD technical resource and tools are estimated and acquired respectively.
  - Risk analysis due to DfD and subsequent appropriate risk management plans are developed.
  - Demisability engineering specialty plans are prepared.
  - Demisability during uncontrolled reentry is included in the mission safety and assurance plans.
  - Technology development plans contain provisions to develop the necessary DfD technology.
  - MDR preparations fully address demisability as a post-mission disposal option.
- **Phase B:** (Preliminary Design and Technology Completion)
  Design-for-Demise practices are engaged in the mission preliminary design concept which details; mission top level performance requirements, and a complete set of system and subsystem design specification. Consequently:
  - Progress related to DfD technology maturity, risk analysis, mission safety and assurance is updated.
  - Top-level requirements finalized and flowed down to the next level address demisability and uncontrolled reentry requirements.

- Validation plans, design drawings, baseline specifications, and interface documents to lower levels established include DfD specifications.
- Further trade studies wholly address demisability.
- The favoured solution includes demisability and uncontrolled reentry where appropriate.
- Preliminary orbital debris and post-mission disposal analysis reports have spacecraft demisability analysis included.
- PDR preparations further serve to escalate demisability and uncontrolled reentry as an option to be adopted in post-mission disposal.

- **Phase C:** (Final Design and Fabrication)
  Design-for-Demise practices are part of the complete detailed design of the mission system and associated subsystems. The fabricated hardware will be demisable wherever possible, therefore:
  - All updates of engineering specialty plans,requirements, baseline and interface documents developed in **Phase B** address the demisability issue.
  - Developed hardware detailed designs include designing hardware parts for demise.
  - Production plans and integration procedures include designing hardware parts for demise.
  - Manufacturing and assembly plans and procedures include designing hardware parts for demise.
  - Verification and validation plans include tested hardware for demise.
  - Trade-offs on the various hardware Design-for-Demise methods are carried out.
  - Demisable hardware parts are fabricated.
  - Demisable hardware parts are part of the testing at the component or subsystem level.
  - Prepared mission decommissioning/disposal plan details demise during uncontrolled reentry as the adopted post-mission disposal approach wherever possible.
  - CDR preparations prove demisability and uncontrolled reentry as the optimal option to be adopted in post-mission disposal.

- **Phase D:** (System Assembly, Integration and Test, Launch)
  The demisable fabricated parts are assembled, integrated and tested to develop confidence in the system meeting stipulated requirements. Moreover, the spacecraft will be capable of withstanding launch conditions and be readied for operations. Consequently:

  - Integration and verification should be conducted according to the earlier developed plans accommodating demise capability.
  - All system assembly, integration and test procedures maintain demisability capability at all levels.
  - Documentation of lessons learned during DfD implementation is done.
  - Integration of spacecraft with launch vehicle and launch are carried out and a deployed system achieved.

- **Phase F:** (Closeout)
  The post-mission disposal plan developed in **Phase C** is implemented and the spacecraft will be disposed via uncontrolled reentry and should completely demise as planned. Collected debris, if any, verifies demisability success and lessons learnt are documented.

The proposed approach will guarantee demisability due consideration for DfD inclusion in all mission life-cycle phases, hence, the opportunity for the mission to benefit from the DfD advantages given in section 1.2 will not be overlooked. The Key Decision Points include DfD benchmarks that have to be satisfactorily met before the mission proceeds to the next phase. It is important to note that not all reentry missions will be demisable even after all possible alternative designs have been considered. This scenario is explicit in Figure 2.5 which shows the proposed execution of DfD practices. The *Critical Parts Identification* process identifies components that directly contribute to the spacecraft non-demisability as further described in Section 3.2.2. Similarly, preliminary and final reentry survivability is done using DAS and ORSAT respectively. DfD realization methods described in Section 5.1.1 are implemented until demisability is achieved or until no further DfD changes can be incorporated hence demisability remains unachieved.

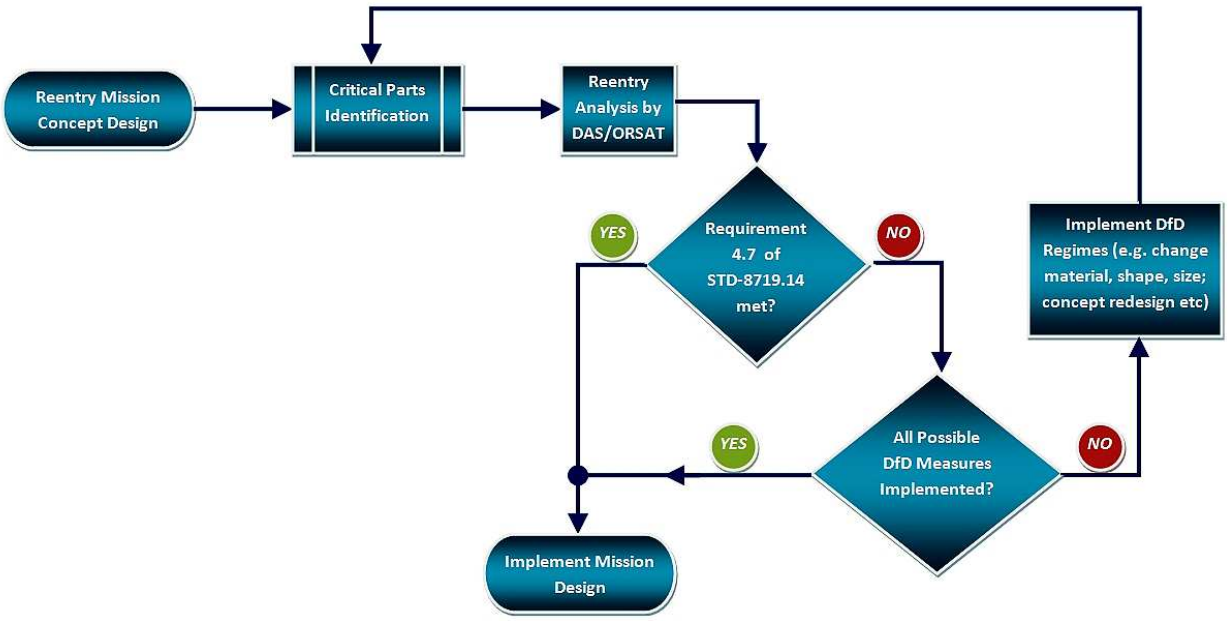

Figure 2.5: Proposed Design-for-Demise execution strategy.

2.5 Chapter Summary

This chapter charted a strategy for the implementation of Design-for-Demise in the formulation and development of reentry LEO space missions. A formal definition of Design-for-Demise was presented then material thermo-physical properties and dynamic thermal environment necessary for demise (ablation) examined. Secondly, classification of reentry LEO missions according to the nature of their function revealed that designing LEO reentry missions for demise is independent of the mission function. Demisability can be integrated in all the five categories of missions identified i.e. *a*) Earth Observation Missions, *b*) Communication Missions, *c*) Space Exploration Missions *d*) Pre-crewed Missions, and *e*) Technology Test Missions . Thirdly, a contrast was established between the previous NASA approach to executing DfD in reentry mission life-cycle and the proposed technique to entrench DfD in reentry mission life-cycle. Unlike the previous NASA approach, the proposed procedure embeds DfD practices in all the formulation phases of the mission life-cycle. The hardware DfD methods are continuously implemented until debris survivability analysis by DAS and ORSAT reveal spacecraft demisability and subsequent compliance to Procedural Re-

quirements and Process for Limiting Orbital Debris[13, 1]. If DfD is adopted during all the developmental phases of any viable reentry LEO mission, the following two objectives will be met: *a*) desired demise altitude upon uncontrolled atmospheric reentry by the spacecraft and *b*) compliance with NASA's orbital debris mitigation policy outlined in NASA's Procedural Requirement 8715.6A - *Limiting Orbital Debris* [13]. Finally, the GPM mission presently in formulation is addressing DfD comprehensively and this thesis aims to contribute towards this effort.

Chapter 3

Analytical Techniques

The tools, procedure and outcome associated with studying demisability of atmospheric reentering objects are discussed in this chapter. We must ascertain the demisability of an object before we determine whether to redesign the object for demise or not. Consequently, we scrutinize reentry analysis tools by examining their general structure, inputs, and outputs. Specific examples of reentry analysis tools are presented, and DAS is scrutinized more deeply. It is important to decompose the spacecraft into basic parts, and a generic effective approach to achieve this decomposition is presented. Decomposing the spacecraft into basic parts specifically facilitates reentry analysis by identifying 'critical' (non-demisable) components. Typical reentry analysis results and their meaning will also be described. Therefore, in examining the analytical techniques in Chapter 3, we shall cover the analysis tools, generic spacecraft subdivision followed by critical parts identification; and finally reentry analysis and interpretation of reentry analysis results.

3.1 Reentry Demisability Analysis Tools

Reentry analysis tools investigate breakups, temperature history and demisability of objects reentering Earth's atmosphere. They are composed of several routines that determine (among other quantities), the object ballistic coefficient, average heating rates, and temperature at each time step in a simulated Earth reentry trajectory. Further, at the end of the trajectory, a progressive world population module and human risk analysis model predict the risk of human casualty on the ground. Consequently, demisability is one of the various

Table 3.1: Stracture of Reentry Analysis Tools.

	Reentry Analysis Modules
1	Spacecraft Definition
2	Reentry Trajectory and Aerodynamic
3	Aero-thermal and Thermal
4	World Population
5	Ground Impact Risk Analysis

functions reentry analysis tools are capable of performing. The reentry analysis method employed can either be object oriented; which analyze the individual parts of a spacecraft, or spacecraft oriented; which model the complete spacecraft as close as possible to the real design. Examples of object oriented reentry analysis tools are Debris Analysis Software (DAS), Object Reentry Survival Analysis Tool (ORSAT) and Spacecraft Entry Survival Analysis Module (SESAM) developed by the European Space Agency (ESA) [15]. An example of spacecraft oriented tool is ESA's Spacecraft Atmospheric Re-entry and Aero-thermal Breakup (SCARAB). In general, the structure of reentry analysis tools can be summarized into five modules as shown in Table 3.1 [10, 16, 17, 18, 19, 20].

Spacecraft Definition Module: This module is populated with the list of all critical individual objects constituting the spacecraft and their corresponding physical properties. The physical properties normally include object mass, shape, material and dimensions. This data is used in conjunction with a material properties database similar to one briefly given in Table 2.1 to analyze demisability; in addition, material density is used to verify integrity of entered data and calculate further object physical properties such as cross-sectional area, volume, and area-to-mass ratios. Moreover, objects may be defined to encapsulate other objects. DAS for instance allows the objects to be defined as containing other objects up to four levels.

Reentry Trajectory and Aerodynamic Module: The Reentry Trajectory module simulates the reentry trajectory via a number of ways: *i)* computing a 3-degree of freedom (point mass motion) or 6-degree of freedom (including attitude motion) trajectory within an Earth-

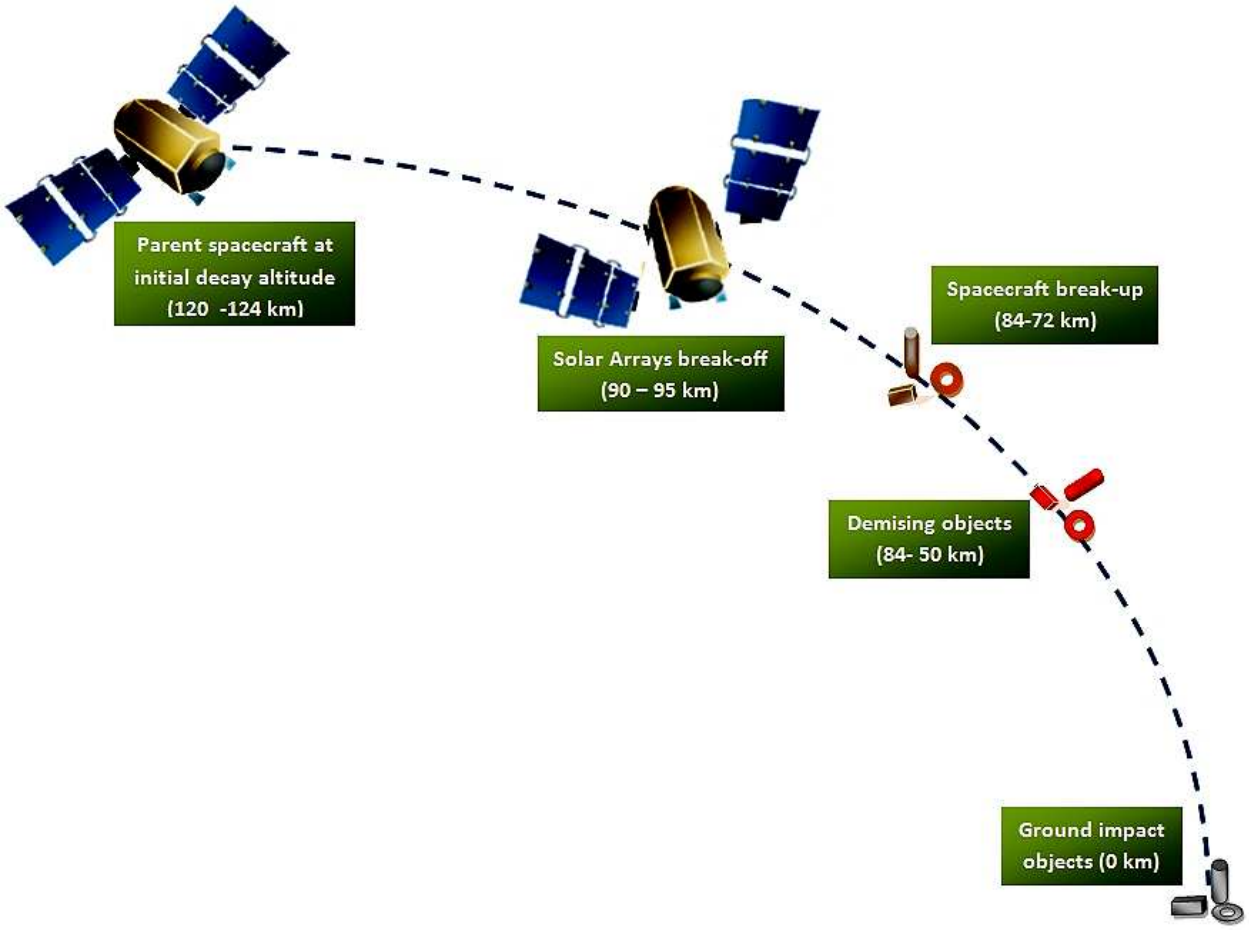

Figure 3.1: Reentry trajectory concept.

fixed reference frame assuming a spherical, rotating Earth [16, 20] adopted from derivations by Allen-Eggers [21, 22] and Dormand-Prince [16]; *ii)*computing six scalar equations that solve the time derivatives of velocity, flight path angle, altitude, longitude, latitude, and heading angle based on derivations by Vinh [17, 23]. Unlike in the former, the latter allows calculation of forces that may cause the flight path to deviate from the great circle plane which is assumed in the former case. These forces can be aerodynamic, atmospheric or gravitational in nature. The perturbation model incorporated typically comprises of Earth gravity field up to J_2 term. The concept of Earth reentry trajectory is illustrated in Figure 3.1.

A standard Global Reference Atmospheric Model is also incorporated. Within it, the

atmospheric density is a function of geodetic altitude $\rho(H)$, relative to an oblate Earth. The aerodynamic modules compute average drag coefficient for cylindrical, spherical, boxes, and flat objects with equations developed from [17, 24]. Moreover, other computed quantities include: elapsed flight time, covered ground distance, velocity, flight path angle, geodetic altitude, latitude and longitude.

Aero-thermal and Thermal Module: The Aero-thermal Module considers the following shapes in motion (spinning and tumbling); spheres, cylinders, boxes, and flat panels when evaluating heating rates due to the interaction between the reentering object's surface and the atmosphere. The equations employed are based on theory developed by Fay and Riddell, which was later extended by Detra, Kemp, and Riddell [16, 25]. As mentioned in Section 2.1, the net heating on the object is given by the sum of convective, radiative and chemical heating less the radiative cooling [10]. Reentry analysis tools may also consider the heat balance for a re-entry object to be governed by incoming aerothermal heating, and heat rejection through radiation only.

In addition, a Thermal Module may consider two-dimensional thermal math models for cylinders and spheres to define temperature in the radial and circumferential direction for reentering objects. These options are used to predict when shells are breached in reentry [17]. The heating analysis assumes that the objects were released from their protective spacecraft shroud at an altitude of approximately 78 km. The surviving objects' cross sectional area and KE energy are computed.

World Population Module: A progressive global population database that gives the average population per km^2 under a spacecraft as a function of inclination and year of entry is included in reentry analysis tools. This is essential in order to assess reentry related risk for a population in an impact ground swath. A satellite's orbital inclination determines the amount of time it spends over each geographic latitude band [26], since each latitude band has a different number of people in it, the number of people under the satellite will vary with time and latitude. The inclination and year of reentry are used in tables to interpolate for the population density. ORSAT, for example, carries out the results to the year 2050 [18], while [16] uses data from the Global Demography Project 1994 that assumes a uniform, proportional growth.

Ground Impact Risk Analysis Module: The ground risk analysis explained in section 1.2 is computed after the total debris casualty area for a particular satellite reentry is obtained. The interpolated population density from the population module is multiplied by the debris casualty area. This information is used to compute the risk of hitting someone on the ground [18, 26].

$$Casualty\ Expectation = Population\ Density \times Casualty\ Area \tag{3.1}$$

The probability (i.e. 'one in N', or '1:N') of a surviving object striking a person is the reciprocal of the casualty expectation.

3.1.1 DAS

The Debris Assessment Software (DAS) is an orbital debris assessment software tool developed by the Orbital Debris Program Office at NASA Johnson Space Center Houston, Texas. DAS assists NASA space programs in performing orbital debris assessments according to the guidelines in NASA Technical Standard 8719.14 - *Process for Limiting Orbital Debris* [1]. NASA Technical Standard 8719.14 sets forth requirements for limiting orbital debris as stipulated in NASA Procedural Requirement 8715.6A - *Limiting Orbital Debris* [13] that requires evaluation of, and minimization of orbital debris generation by NASA programs. DAS provides the outline and format for preparing Orbital Debris Assessment Reports to be submitted at key decision points; Preliminary Design Review, and shortly before the Critical Design Review. If the space program is non-compliant to the requirements, DAS may also be used to explore debris mitigation options to realize compliance [8]. The current version of *DAS 2.0.1* is available for download from the NASA Orbital Debris Program Office website [27].

DAS functionality structure can be chiefly divided into the following parts: *a*) **Mission Editor**, *b*) **Requirement Assessment**, *c*) **Material Database** and *d*) **Science and Engineering Utilities** [8].

Mission Editor

The Mission Editor enables the definition of spacecraft, rocket bodies, and mission related debris (as outlined in section 3.1) for orbital debris requirement assessments. Among other

mission properties, a user is able to define launch year, mission duration, mission components, and orbital characteristics as shown in Figure 3.2.

Requirement Assessment

The Requirement Assessment utility contains a list of supported requirements from NASA Technical Standard 8719.14 - *Process for Limiting Orbital Debris* [1] to be adhered to. Mission data entered in the Mission Editor is analyzed against each requirement and it is compliance status subsequently determined and presented. See Figure 3.2.

Material Database

The editable Material Database stores material information used in the reentry demisability analysis of an object. The three material thermo-physical properties used in analysis of an object's reentry demisability: specific heat, heat of fusion, and melt temperature are concurrently given (see Section 2.1). A user is able to create additional materials absent from the material database. Each additional entry must define the three above mentioned thermo-physical properties and the material density. DAS uses material density to make sure a component's mass and size are consistent.

Science and Engineering Utilities

The Science and Engineering Utilities analyze aspects of the missions design outside the context of Requirement Assessments. It is this part of DAS that is of interest to us in carrying out Design-for-Demise analysis. Below is the list of Science and Engineering Utilities found in DAS:

- On-Orbit Collisions
- Analysis of Post-mission Disposal Maneuvers
  - Disposal by Atmospheric Reentry
  - Maneuver to Storage Orbit
  - **Reentry Survivability Analysis**
- Orbit Evolution Analysis
- Delta-V for Post-mission Maneuver

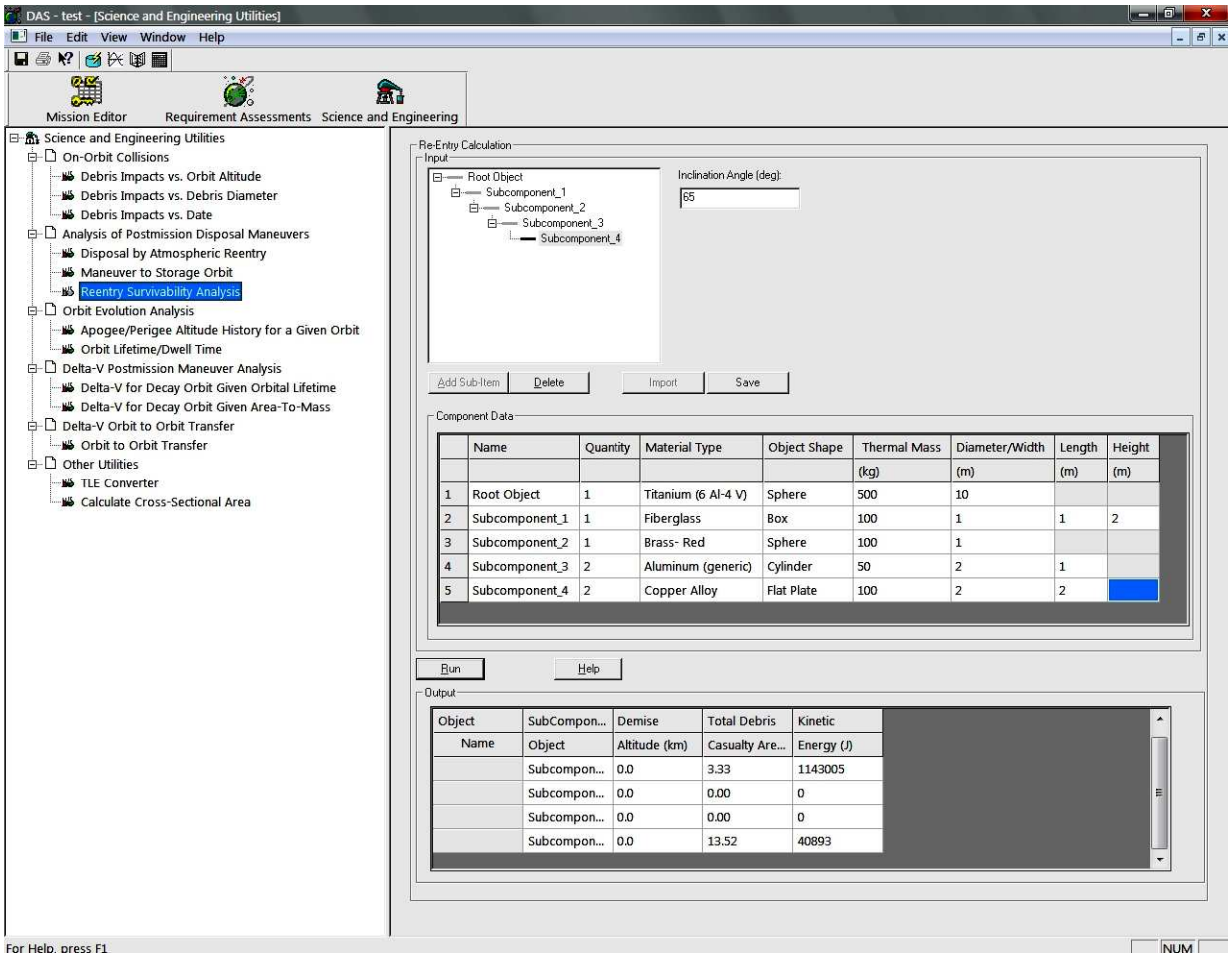

Figure 3.2: *DAS 2.0.1* Mission Editor, Requirement Assessment, Science and Engineering Utilities, and Reentry Survivability Analysis utility.

- Delta-V for Orbit-to-Orbit Transfer

We use the above highlighted **Reentry Survivability Analysis** utility in analyzing the demisability of a given object. Figure 3.2 shows the Reentry Survivability Analysis model and the other DAS components.

DAS 2.0.1 Reentry Survivability Analysis uses a simplified version of ORSAT to determine demisability of objects during reentry which determines thermal heating based on a lumped mass approach [20]. This utility allows for reentry analysis without changing the mission characteristics as entered in the Mission Editor because the reentry spacecraft is

re-defined independently. Apart from the the specification of orbital inclination, up to 200 unique hardware components can be entered in up to four nested levels. The outermost structure ('parent') object is assumed to break apart at an altitude of 78 km exposing the first level of 'child' objects to the forces of the reentry model. Subsequent 'child' objects are similarly exposed at the same point at which their immediate parent object demises. This progressive exposure of nested structures allows DAS to model a more accurate and realistic reentry scenario.

DAS Reentry Survivability Analysis utility accepts the mission orbit inclination and the following object properties: shape (sphere, cylinder, box and flat panel); dimensions (diamater, width, length, and height); material type, and thermal mass. Thermal mass of an object is the object mass without including the mass of defined sub-components; it is the mass of the 'parent' structure. The Reentry Survivability Analysis utility gives the following results for each defined subcomponent:

Demise Altitude: The predicted object altitude at which complete ablation occurs. A demise altitude of 0 km indicates non-demisability and the object is expected to impact the ground.

Kinetic Energy: The kinetic energy of impacting objects in Joules. Only objects with kinetic energy above 15 Joules are displayed.

Total Debris Casualty Area: The Debris Casualty Area for a piece of surviving debris is the average debris cross-sectional area plus a factor for the cross-section of a standing individual. Consequently the Total Debris Casualty Area is the sum of the debris casualty areas for all individual reentry surviving objects. Equation 3.2 computes the Total Debris Casualty Area [1].

$$D_A = \sum_{i=1}^{N} \left(0.6 + \sqrt{A_i}\right)^2 \tag{3.2}$$

Where:
N = number of objects surviving reentry.
A_i = Area of object surviving reentry.
0.6 = square root of average cross-sectional area of a standing individual viewed from above which is taken to be 0.36 m^2.

DAS Limitations

The DAS Reentry Survivability Analysis utility is a relatively moderate fidelity tool designed for individuals who are not necessarily reentry physics specialists. It hence contains some simplifications and a small amount of conservatism which compromises its fidelity. Nevertheless, *DAS 2.0.1* philosophy is that if DAS analysis shows compliance with the NASA casualty requirement of 1 in 10,000, then no further analysis is required. However, if the DAS analysis show non-compliance with this requirement, further analysis by higher fidelity tools like ORSAT is required. Though not an exhaustive list, some of the *DAS 2.0.1* limitations due to simplifications and conservatism include:

- Concerns related to controlled reentry *(Requirement 4.7-1.b)* are not addressed [1].
- Assumption of initial 'parent' object breaking up at one altitude of 78 km which neglects different exposure times and altitudes for the modeled objects [28].
- Assumption of initial 'parent' object breaking up at one altitude of 78 km means that DAS would generally predict a higher ground risk.
- Heating at altitudes above 78 km is ignored in *DAS 2.0.1.*
- Neither pre-heating of internal structures nor partial ablation is included. Consequently, each 'child' object is exposed with the same starting temperature (300 Kelvin). The lack of partial ablation means that an exposed structure's cross sectional area is either zero (demised) or is the usual product of the initial dimensions.
- Since DAS is not able to predict partial ablation, this is a more conservative approach to human casualty risk assessment, which is a function of total debris casualty area.
- All material properties in DAS are assumed to be temperature independent.
- DAS assumes a constant emissivity of 1.0 for all materials [20].

Finally, other DAS utilities include *a*) *Two Line Element Converter* that converts data related to orbital mechanics into orbital parameters that can be used in DAS, and *b*) *Calculate Cross-Sectional Area* which assists users in estimating the effective cross-sectional area of a structure.

3.1.2 ORSAT

The Object Reentry Analysis Survival Tool (ORSAT) is a more complex and comprehensive reentry analysis tool with higher fidelity assessment of thermal destruction during ballistic reentry than DAS. Like DAS, ORSAT evaluates the human casualty risk due to reentering spacecraft and launch vehicle upper stages according to guidelines in NASA Technical Standard 8719.14 - *Process for Limiting Orbital Debris* [1], and requirements stipulated in NASA Procedural Requirement 8715.6A - *Limiting Orbital Debris* [13]. ORSAT predicts the debris casualty area (DCA) of reentry objects based on their size, body shape and motion assumptions. Then, ORSAT uses DCA to determine the reentry risk posed to the Earth's population based on the year of reentry and orbit inclination. It also predicts impact kinetic energy (impact velocity and impact mass) of objects that survive reentry[18]. ORSAT has been in use for the last decade and currently in its 6.0 version. However, unlike DAS, ORSAT is not readily available. Only personnel at the Johnson Space Center, Orbital Debris Program Office run ORSAT. ORSAT is limited to ballistic reentry, only tumbling motions or stable orientations of objects are allowed which produce no lift. Partial melting of objects is considered by a demise factor and almost all materials in the database are temperature dependent. Heating by oxidation is also considered [20]. Therefore, ORSAT determines when and if a reentry object demises by using integrated trajectory, atmospheric, aerodynamic, aero-thermodynamic, and thermal models as outlined in section 3.1 [17, 18, 20].

3.2 Reentry Demisability Analysis

Reentry demisability analysis using DAS requires the spacecraft to be defined to the level of each individual hardware part constituting the spacecraft. This step facilitates population of the DAS *Spacecraft Definition Module* . Section 3.2.1 illustrates a generic spacecraft subdivision approach that can be followed to itemize the individual parts spacecraft parts. Subsequently, non-demisable parts are identified before or by the actual reentry analysis as explained in section 3.2.2.

Table 3.2: Generic decomposition of Structure & Mechanisms and, Propulsion subsystems.

Subsystem	Assembly	Subassembly	Part
Structure and Mechanisms	Launcher/Spacecraft Interface	Marmon Clamps	Marmon Clamps
		Separation Bolts	Separation Bolts
	Primary Structure	Spacecraft bus	Bus components
	Secondary Structure	Brackects	Brackect
		Closeout panels	Closeout panel
		Boom appendages	Boom appendage
	Mechanisms	High Cycle Applications	Antenna Gimbals
			Solar Array Drives
			Boom Extensions
		Low-Cycle Applications	Subassembly Retention-mechanisms
			Subassembly Release-mechanisms
			Subassembly-Deployment-mechanism
			Contamination cover removal
	Deployables	Deployment Hinges	Deployment Hinges

Subsystem	Assembly	Subassembly	Part
Propulsion	Propellant	Cold Gas	Cold gas
		Chemical	Liquid: Monopropellant
			Liquid: Bipropellant
			Liquid: Tripropellant
			Liquid:Dual Mode
			Liquid: Water Electrolysis
			Solid
			Hybrid
		Electric	Electrothermal
			Electrostatic
			Electromagnetic
		Nuclear	Nuclear reactor
	Engine	Thrusters	Thrusters
		Motors	Motors
		Resistojets	Resistojets
		Arcjets	Arcjets
	Tanks	Tanks	Tank
	Lines, Valves and Fittings	Lines, Valves and Fittings	Line, Valve & Fitting

3.2.1 Generic Spacecraft Subsystems Hierarchical Subdivision

Itemization of the demisable spacecraft basic parts can be best approached by decomposing the spacecraft according to the Hierarchical System Terminology defined in the NASA Systems Engineering Handbook [14]. Tables 3.2, 3.3 and 3.4 illustrate a generic approach to decompose a spacecraft into basic parts [29, 30, 9] excluding the payload. Description of the specific product for the basic part identified completes the process. Though slight variations are likely to occur in the decomposition of different missions, the *Generic Spacecraft Subsystems Hierarchical Subdivision* approach is robust, hence, will ensure an efficient and comprehensive collapse of the candidate spacecraft into it's basic parts. Other approaches may be utilized as the demisability analysis team deem fit for the particular mission analysis at hand.

Table 3.3: Generic decomposition of ADC, TT&C, Power and, GNC spacecraft subsystems.

Subsystem	Assembly	Subassembly	Part
Attitude Determination and Control (ADC)	Attitude Measurement	Coarse Attitude Sensors	Coarse Magnetometers
			Sun Sensors
			Earth Horizon Sensors
		Precise Attitude Sensors	Fine Sun Sensors
			Star Sensors
			Gyroscopes
			Accelerometers
			GPS Receivers
	Attitude Control	Active Attitude Control	Momentum wheel
			Control Momentum Gryos
			Reaction Wheel Assembly
			Jets
			Magnetic Torquers
			Thrusters
		Passive Attitude Control	Gravity Gradient Boom
	ADC Processing	ADC Processing	Attitude Processing Electronics

Subsystem	Assembly	Subassembly	Part
Power	Power Generation	Solar Panels	Photovoltaic cells
		Static Power Sources	Radioisotope TG
			Nuclear reactors
		Dynamic Power Sources	Brayton Cycle
			Rankine Cycle
			Stirling Cycle
		Chemical Power sources	Fuel Cells
	Power Storage	Primary Battery Cells	Silver Zinc
			Lithium Thionyl Chloride
			Lithium Sulfur Dioxide
			Lithium Monoflouride
		Secondary Battery Cells	Nickel-Cadmium
			Nickel-Hydrogen
			Nickel-metal hydride
			Lithium-Ion
			Sodium-Sulfur
	Power Distribution	Cabling	Copper cables
		Fault Protection	fuses, Circuit Breakers
		Switching Gear	Mechanical/solid state relays
	Regulation and Control	Regulation	Shunt Regulator
			Series Regulator
			Shorting switching array
		Control	Power Processing Electronics

Subsystem	Assembly	Subassembly	Part
Telemetry Tracking and Control - TT&C (Communication)	Carrier Tracking & Ranging	Transponder	Receiver Circuitry
			Amplifier Circuitry
			Transmitter Circuitry
		Amplifier	Solid State Amplifier
			Travelling Wave Tube Amplifier
		Antennae	Parabola
			Turnstile
			Hemispherical
			Waveguide
	Command Reception & Detection	Command Reception	Command Reception Processors
		Command Detection	Command Detection Processors
	Subsystems Operations	Subsystem Commands	Subsystem Command Processors
		Antennae Pointing	Antennae Pointing Processors
		Fault Recovery	Fault Recovery Processors

Subsystem	Assembly	Subassembly	Part
Guidance Navigation and Control – GNC	Guidance and Navigation	Real-time Orbit Determination	Real-time Orbit Determination Circuitry
		Definitive Orbit Determination	Definitive Orbit Determination Circuitry
	Navigation Sensors	Altitude Sensing	Altitude Sensors
		GPS Receivers	GPS Receiver
		Earth sensing	Earth Sensor
		Star Sensing	Star Sensor
	Control	Propulsion	Thrusters

Table 3.4: Generic decomposition of Thermal Control and, Command & Data Handling spacecraft subsystems.

Subsystem	Assembly	Subassembly	Part
Thermal Control	Passive Thermal Control	Materials	Ag, Al -baked teflon
			Multi-layer Insulation
		coatings	White/Black paint
			Al foil
			Gold plating
		radiators	Structural Panels radiators
			Flat-plate radiators
		Heat Pipes	Heat Pipes
		Surface Finishes	second surface mirrors
	Active Thermal Control	Heaters	Patch heaters
			Cartridge heaters
		Louvers	Louvers
		Thermoelectric Coolers	Thermoelectric Coolers

Subsystem	Assembly	Subassembly	Part
Command and Data Handling (C&DH)	Command	Central Processing Units	CPU microchip
		Antennae	Turnstile
			Hemispherical
		Receiver/Demodulator	Receiver/Demodulator Circuitry
		Command Decoder	Command Decoder Circuitry
		Interface Circuitry	Interface Circuitry
	Data Handling	Memory	ROM, RAM
		Mass Storage	Tape, Solid State
		Data Input/Output	Ports, Bus interface

3.2.2 Critical Parts Identification

Knowledge of non-demisable spacecraft hardware parts is key to the Design-for-Demise process. We refer to the non-demisable parts as *Critical Parts*. After identifying the *Critical Parts*, DfD regimes as described in Section 5.1.1 can then be employed. Two ways of identifying *Critical Components* are *a*) Prior knowledge and *b*) Reentry analysis results.

Prior knowledge: One way to identify non-demisable spacecraft parts is through knowledge from previous reentry missions in which the particular parts did not demise. Consequently, the known non-demisable parts and those with similar thermo-physical properties can be avoided during the DfD realization process. The non-demisable parts may also cataloged for future reference. According to [31] more than 18,000 trackable objects reentered the Earth atmosphere since the first space launch in 1957 and up to 2002. These reentered objects have a total cumulative mass of approximately 27,000 tons and a cumulative cross-section area of approximately 85,000 m^2. Moreover, data from reentry objects is used to validate an d calibrate reentry analysis tools. The plot in Figure 3.3 shows the number of tracked objects roughly larger than a basketball that reentered the Earth atmosphere for the years 1957 to 2006. Examples of recovered non-demisable spacecraft parts that have reentered the Earth's atmosphere are pictured in Figure 3.4.

Reentry analysis results: Empirical analysis of reentry objects demisability is achieved by mathematically modeling the interaction between the reentering objects and the dynamic reentry environment along a simulated reentry trajectory. The analytical results obtained as outlined in section 3.2.3 identify *Critical Parts* by predicting the demisability of a given object.

3.2.3 Reentry Demisability Analysis Results

As described in section 3.1.1, the output of the DAS reentry analysis is the demise altitude, kinetic energy and total debris casualty area (for the ground impacting objects). Behavioral trends can hence be established from these results based on object material, size and shape as shown in Figure 3.5 and 3.6.

From the plot in Figure 3.5, we observe and deduce that:

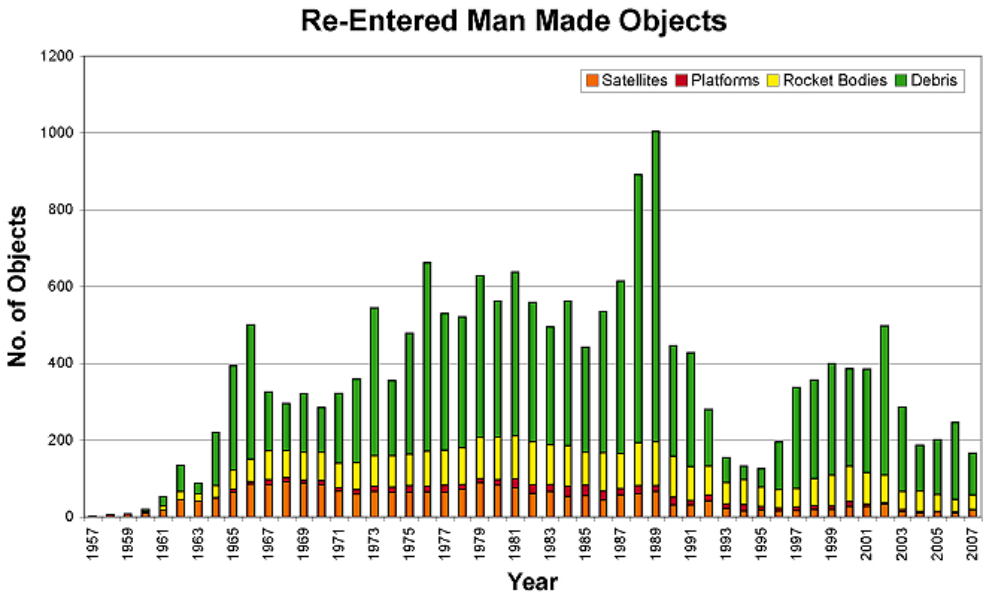

Figure 3.3: Number of tracked, reentered objects roughly larger than a basketball for the years 1957 to 2006. Platforms are used to support a payload while it is being placed into orbit. (Courtesy: The Aerospace Corporation)

Figure 3.4: *a)* A metal plate (2.4 x 2.4 m, mass 20 kg) from Russian Cosmos 2267 satellite found in Cosala, Mexico. Launched 5 November 1993, reentered on 28 December 1994. (Courtesy: www.eclipsetours.com). *b)* Titanium pressure sphere (diameter 0.37 m) from Soviet Foton 4, found in Marble Bar, Australia. Launched 14 April 1988, reentered 28 April 1988. (Courtesy: www.space.com)

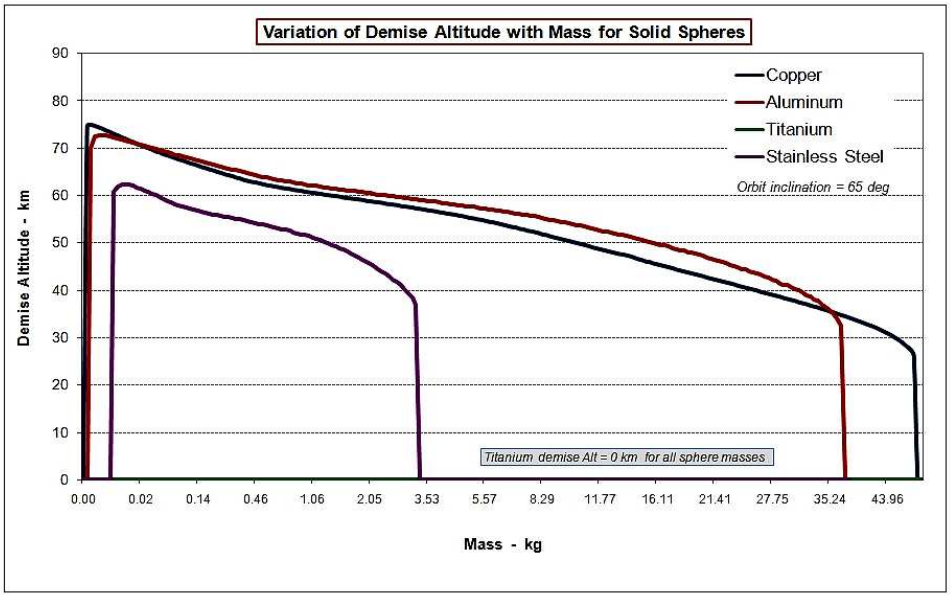

Figure 3.5: How the demise altitude varies with changing mass of solid spheres in *DAS 2.0.1* analysis

- Ti impacts the ground for all the different diameters, however, for Cu, Al and stainless steel, each material demises for a certain range of diameter beyond which it impacts the ground.

- Even though a material (e.g. Al) may have a low melt temperature, area-to-mass ratio can make them non-demisable due to their rapid deceleration in the upper atmosphere. Hence the behavior exhibited at the beginning of the plots (low mass).

- Increasing the mass of an object also raises its KE due to the corresponding rise in terminal velocity.

- The inclination is used to compute the Expected Human Casualty Risk evaluated as a product of the Population density (along the orbit) and the Total DCA.

The objects in consideration that yield the plots shown in Figure 3.6 are not solid structures. DCA is computed for KE greater than $15J$. Otherwise it is treated as zero. From the plots, we can observe and conclude that:

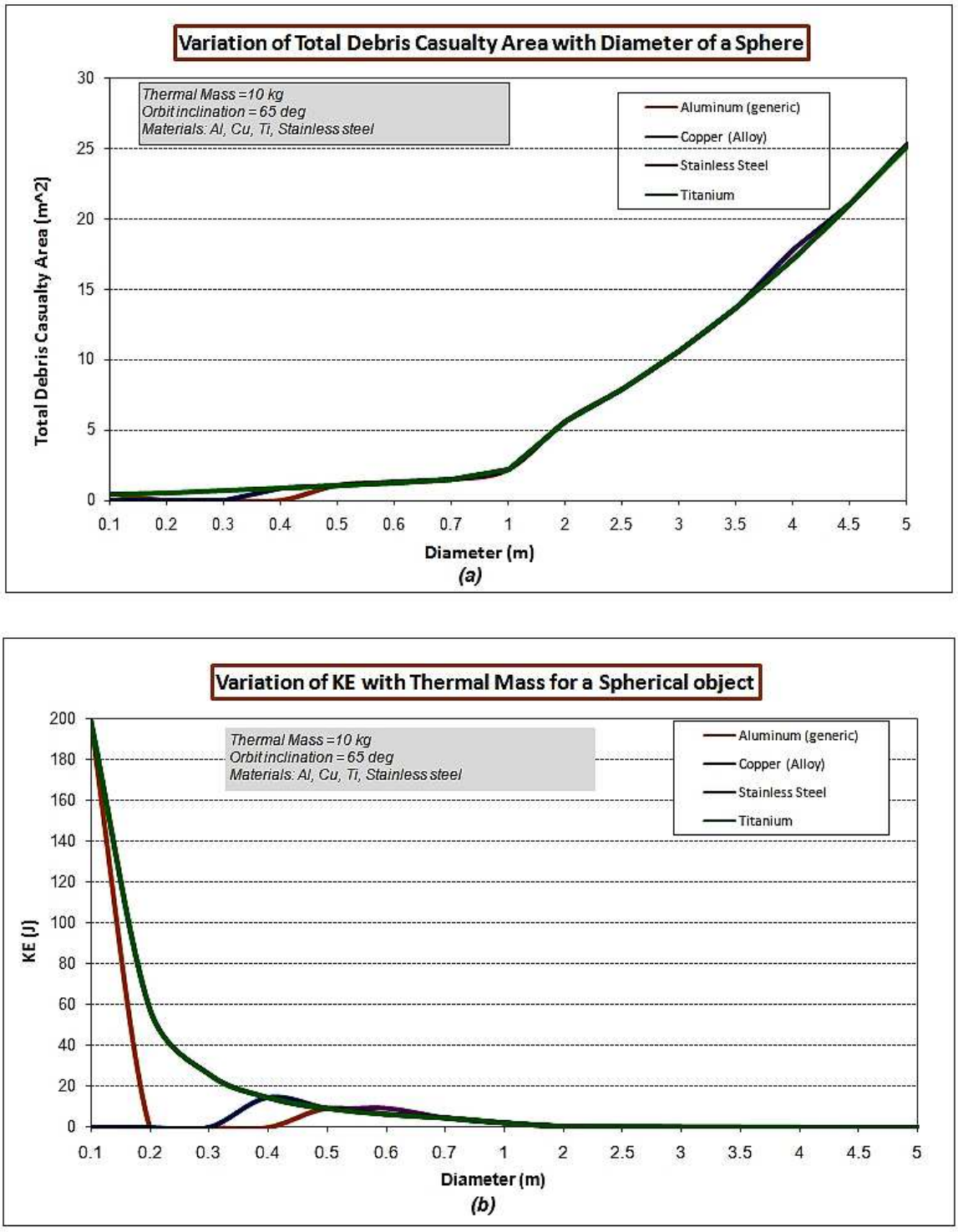

Figure 3.6: How KE and Debris Casualty Area varies with changing diameter of spherical objects *DAS 2.0.1* analysis

- All four materials exhibit a gradual increase in DCA as the diameter rises between 0.1 m and 1 m. However a corresponding sharp increase in DCA is noticed beyond the 1 m point of diameter.
- DCA is increases with increase in diameter because it is a function of the object cross section area. The object cross-section area is directly a function of the increasing diameter
- Increasing the diameter while holding the Thermal Mass constant implies shrinking the structure walls to accommodate the corresponding enhancing breadth.
- As the object diameter increases, its KE declines due to a relatively larger x-section area being exposed to the dynamic aerothermal ablation environment. In turn, relatively lower subsequent thermal masses result in relatively lower terminal velocity , hence a declining KE value.

3.3 Chapter Summary

Chapter 3 investigated how to carry out reentry demisability analysis and the tools employed in the reentry analysis process. We presented four main reentry analysis tools; DAS, ORSAT, SCARAB and SESAM with a detailed description of DAS. Further, we established that the structure of reentry analysis tools can be generically divided into the following five main parts: *i*) Spacecraft Definition *ii*) Reentry Trajectory and Aerodynamic *iii*) Aero-thermal and Thermal *iv*) World Population and, *v*) Ground Impact Risk Analysis. We undertook a deeper scrutiny into DAS because we use it in our demisability analysis. In order to effectively predict spacecraft demisability using reentry analysis tools, we presented a generic hierarchical approach to itemize the spacecraft basic parts. This was followed by identification of critical parts that are non-demisable. After identifying critical components, hardware DfD methods will be executed to achieve demisability. Finally, we outlined typical DAS reentry analysis results and demonstrated how to interpret and draw conclusions from the results.

Chapter 4

Design-for-Demise Decision-Making Methodology

Here, we shall present a decision making facilitation framework to aid in the decision to design a spacecraft for an uncontrolled reentry post-mission disposal option. A deeper scrutiny into the process execution and characteristics of its components will be carried out here. As part of this effort, we shall explore the various aspects that affect a given space mission in general.

4.1 Analytic Deliberative Decision-Making Process

To facilitate the decision to design for demise, we propose the The Analytic Deliberative Decision-Making Process (ADP). This process is similar to the decision-making process suggested by the risk assessment and analysis group at MIT for the NASA Lunar Surface Systems-Payload Handling System. ADP involves *analysis* and *deliberation*. It brings together the decision maker, experts and stakeholders in a decision-making process that embraces information organized in a manner that distinguishes benefits and risks associated with candidate decision options. Moreover, ADP keeps track of uncertainty and aggregates both objective and subjective information while assisting in the systematic identification of objectives of making a particular decision and the respective associated performance options. At the core of the ADP is the hierarchical collection of all elements that the decision maker, experts and stakeholders believe to be important in evaluating the decision options [32]. This

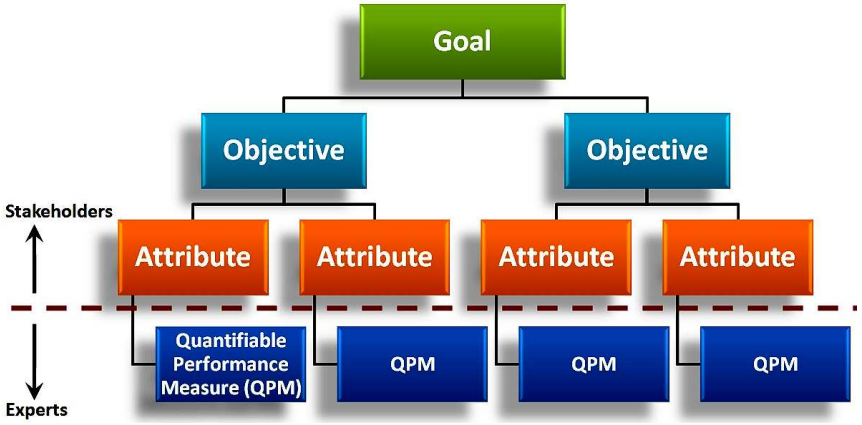

Figure 4.1: Schematic Objectives Hierarchy

information is captured by forming an Objectives Hierarchy, as shown in Figure 4.1 [33].

Goal: Statement explaining the overall purpose of making the decision.
Objectives: Broad categories of elements that the stakeholders feel need to be achieved in order for a decision option to meet the goal.
Attributes: The most detailed level of sub-objectives which describe how to achieve the objectives above them.
Quantifiable Performance Measures: Specify the extent to which an option satisfies an attribute by reporting the level of performance of each option with associated uncertainty.

The formulation of QPMs is followed by determining how relatively important each attribute is to achieving the overall goal using the Analytic Hierarchy Process (AHP). AHP involves pairwise comparison of attributes, and then objectives by each individual. Further, each individual must choose which of the pair is more important to achieving the goal.

After all the information has been collected, preliminary ranking of each decision via the Performance Index (PI) is done. PI can be determined for each decision option as shown in Equation 4.1.

$$PI_j = \sum_{i=1}^{N_{PM}} w_i v_{ij} \tag{4.1}$$

Where:

Figure 4.2: Reentry post-mission disposal options.

PI_j = PI for alternative j.
v_{ij} = values associated with the QPMs for attribute i determined by AHP.
w_i = APH determined weight for attribute i.

The effect of uncertainty is shown for the decision options that are ranked according to their expected PI calculated separately for each stakeholder and decision maker. Deliberations between individual stakeholders and the decision maker over their rankings leads to a collective decision. Though ADP does not produce one best decision, it separates out the components of decision making process, hence facilitating a consensus between the decision maker and the stakeholder [32].

4.2 Post-Mission Disposal Decision Making

NASA Technical Standard 8719.14 - *Process for Limiting Orbital Debris* [1], requires retiring of a space mission at the end of mission lifetime through atmospheric reentry, maneuvering to a storage orbit, or direct retrieval. Atmospheric reentry is the appropriate option for missions passing through LEO considered in this thesis. The three options available for post-mission disposal using the reentry method are schematically shown in Figure 4.2. We shall employ the ADP decision making process for the Demisable Uncontrolled Reentry option since it involves design-for-demise in order to meet NASA post-mission disposal requirements. Specifically, we shall concentrate on the *analysis* phase of the ADP methodology as described in Section 4.2.1, and leave the *deliberative* phase for future work.

The ADP process is also assumed to be employed for the other two reentry post-

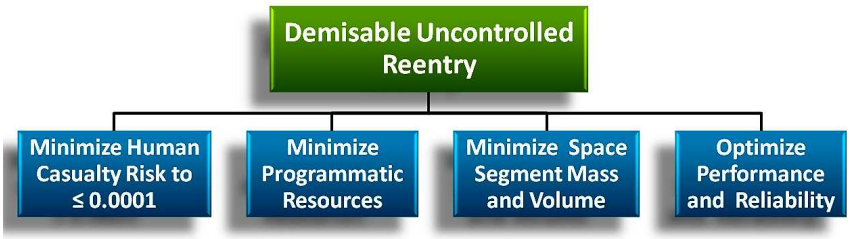

Figure 4.3: Demisable Uncontrolled reentry Goal and Objectives.

mission disposal options: Controlled Reentry and non-Demisable Uncontrolled Reentry with Reentry Requirements Waiver.

4.2.1 Design-for-Demise Objectives Hierarchy

To facilitate realization of the Demisable Uncontrolled Reentry goal, four objectives to be fulfilled are identified as schematically shown in Figure 4.3.

1. **Minimize Human Casualty Risk to ≤ 0.0001**
   The acceptable Human Casualty Risk according to NASA Technical Standard 8719.14 is 1:10,000 (0.0001). Consequently one of the objectives in achieving demisability during uncontrolled reentry is to maintain a casualty risk less than or equal to this value.

2. **Minimize Programmatic Resources**
   Programmatic Resources are finite and limited, hence another objective to realize a demisable uncontrolled reentry mission and further deem this option attractive, is to minimize programmatic resources. The specific attributes of Programmatic Resources are described later in this section.

3. **Minimize Space Segment Mass and Volume**
   Not only is it crucial to design the space-segment to demise for the uncontrolled reentry mission, but in doing so, it is our objective to minimize the mass and volume budgets. This objective will translate into mission financial cost savings.

4. **Optimize Performance and Reliability**
   Mission performance and reliability should not be overly suppressed while designing

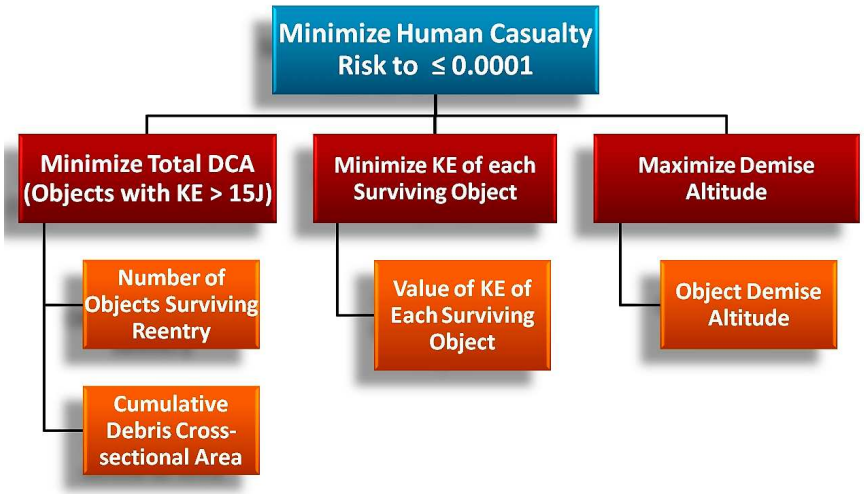

Figure 4.4: Minimize Human Casualty Risk Objectives Hierarchy

uncontrolled reentry missions for demise. On the contrary, as required of virtually all space missions, the demisable design should likewise optimize mission performance and reliability.

After identifying the objectives, we next investigate the associated attributes and QPMs for each objective in a fragmented view.

1. **Minimize Human Casualty Risk to ≤ 0.0001 Objectives Hierarchy**
   Three identified attributes that minimize the Human Casualty risk are *a*) Minimizing Total Debris Casualty Area for non-demisable objects with KE greater than $15J$, *b*) Minimize the KE of each object to $\leq 15J$, and *c*) Maximize the Demise Altitude. The attributes of this objective and corresponding QPMs are schematically given in Figure 4.4.
   Two measurable consequences are identified as QPMs to Minimize Total Debris Casualty Area for non-demisable objects with KE greater than $15J$ - Number of Objects Surviving Reentry and Cumulative Debris Cross-sectional Area.

   - *Number of Objects Surviving Reentry*
     Here, the two extreme performance levels will be determined from the number of non-dimasable objects upon reentry as a percentage function of the total number

Table 4.1: Demisability Performance Levels for Number of Objects Surviving Reentry.

Performance Level	**Value**
100% of spacecraft objects are non-demisable	0
75% of spacecraft objects are non-demisable	0.25
25% of spacecraft objects are non-demisable	0.75
0% of spacecraft objects are non-demisable	1

of objects making the space segment. The lower value of consequence will be 0 which corresponds to 100% of total number of spacecraft objects surviving reentry-essentially, the entire spacecraft survives reentry. The higher value of consequence will be 1 which corresponds to 0% of total number of spacecraft parts surviving reentry-essentially, the entire spacecraft demises. This is the desired scenario. A linear interpolation determines the discrete values at different points within the range of consequence. For example if 25% of spacecraft objects are non-demisable, then the level of consequence will be 0.75 and if 75% of spacecraft objects are non-demisable, then the level of consequence will be 0.25 and so forth. This relation is summarized in Table 4.1.

- *Cumulative Debris Cross-sectional Area*
  Similarly, the cumulative debris cross-sectional area of non-dimasable objects will be determined as a percentage function of the cumulative area of the total number of objects making the space segment. The lower value of consequence will be 0 which corresponds to 100% of cumulative debris cross-sectional area of the spacecraft parts surviving reentry-essentially, the entire spacecraft survives reentry. The higher value of consequence will be 1 which corresponds to 0% of cumulative debris cross-sectional area of spacecraft parts surviving reentry; essentially, the entire spacecraft demises. Similarly, a linear interpolation determines the discrete values at different points within the range of consequence. To illustrate, if 35% of cumulative debris cross-sectional area of spacecraft objects are non-demisable, then the level of consequence will be 0.65 and if 85% of cumulative debris cross-sectional area of spacecraft objects are non-demisable, then the level of consequence will be 0.15 and so forth. This relation is summarized in Table 4.2.

Table 4.2: Demisability Performance Levels for Cumulative Debris Cross-sectional Area.

Performance Level	**Value**
100% of spacecraft cumulative debris cross-sectional area is non-demisable	0
65% of spacecraft cumulative debris cross-sectional area is non-demisable	0.35
15% of spacecraft cumulative debris cross-sectional area is non-demisable	0.85
0% of spacecraft cumulative debris cross-sectional area is non-demisable	1

Considering the *Minimize KE of Each Surviving Object* attribute, we identify the measurable consequence as the value of KE possessed by the ground impacting object as the QPM. According to NASA Technical Standard 8719.14 , only non-demisable objects with $KE \geq 15J$ are considered hazardous. Therefore, the lower value of consequence, 0, will correspond to $KE > 15J$. The higher value of consequence will be 1 which corresponds to $KE \leq 15J$. This particular QPM is an example of a binary switch performance level, the value is either 1 or 0 always.

Finally, in considering the *Maximimize Demise Altitude* attribute, we identify the reentry object demise altitude as the measurable consequence hence it becomes the QPM. Non-demisable objects impacting the ground will have a demise altitude of zero. Reentry objects normally tend to demise an altitude of 84-50 km as described in Section 3.1. Ablation of reentry objects is unlikely to occur below 50 km altitude. However the demise altitude QPM will not take into account the particular altitude the object demises. We will only consider if an object demises or not. Consequently, the lower value of consequence, 0, will correspond to Demise Altitude = 0 km. The higher value of consequence will be 1 which corresponds to Demise Altitude$>$ 0 km. This is also a binary switch performance level.

2. **Minimize Programmatic Resources**
   Three attributes identified to minimize programmatic resources are *a*) Minimizing space segment cost *b*) Minimizing Design-for-Demise impact on project schedule, and *c*) Minimizing Design-for-Demise impact on human resource. The attributes of this objective and corresponding QPMs are schematically given in Figure 4.5.

   Two measurable consequences identified as QPMs to minimize space segment cost are;

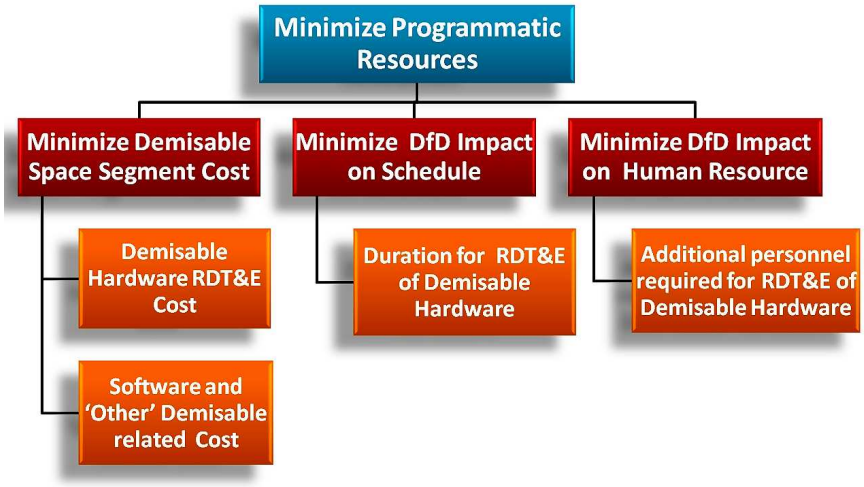

Figure 4.5: Minimize Programmatic Resources Objectives Hierarchy

Demisable hardware RDT&E cost and *Software plus 'other' demisability related costs.*

- *Demisable hardware RDT&E cost*
  Demisable hardware RDT&E costs are additional costs incurred by the project solely due to demisable hardware pursuit. The range of consequence will vary from 0 to 1 as before. The lower value of consequence, 0, corresponds to the cost determined by the project management as the highest possible acceptable demisability RDT&E cost. Therefore the higher level of consequence, 1, will correspond to ideal lowest acceptable demisability RDT&E cost. It is feasible to set this value to zero. A linear interpolation determines the intermediate values of consequence within the 0-1 range. Moreover, the project management can determine the demisability RDT&E cost as a relative function of the entire project RDT&E cost. For example demisable hardware RDT&E cost can be set not to exceed 10% of project RDT&E cost. If it is $1-3\%$ of project RDT&E cost, then it is considered an ideal case. The level of performance will hence vary depending on the project and its management.

- *Software plus 'other' demisability related costs*
  Re-designing the space segment for demise via methods described in section 4.3.1 may involve software reconfigurations and other non-hardware related costs. This

QPM captures such aforementioned costs. Similarly, the range of consequence will be from 0 to 1. The lower value of consequence, 0, corresponds to the cost determined by the project management as the highest possible acceptable demisability software and 'other' costs, and the higher level of consequence, 1, will correspond to ideal lowest acceptable demisability software and 'other' costs.

To minimize Design-for-Demise impact on the project schedule, the measurable consequence identified as the QPM is the *Duration of RDT&E of Demisable Hardware*. This is the additional time required to exclusively develop and qualify demisability capability within the space segment. Similar to demisability RDT&E cost, the range of consequence will be from 0 to 1. The lower value of consequence, 0, corresponds to the duration determined by the project management as the highest possible acceptable demisability RDT&E duration , and the higher level of consequence, 1, will correspond to ideal lowest acceptable demisability RDT&E duration. A linear interpolation determines the values of consequence within the 0 - 1 range. Moreover, the project management can determine the demisability RDT&E duration as a relative function of the entire project RDT&E duration.

Finally, to minimize Design-for-Demise impact on human resource, the measurable consequence is identified as the *Additional Demisability RDT&E Personnel.* This is the additional human resource required solely because of the requirement to redesign parts of the space segment for demise. The range of consequence will be from 0 to 1. The lower value of consequence, 0, corresponds to the demisability RDT&E expertise personnel determined by the project management as the highest possible acceptable, and the higher level of consequence, 1, will correspond to ideal lowest acceptable additional demisability RDT&E expertise personnel.

3. **Minimize Space Segment Mass and Volume**
   Two attributes identified to minimize space segment mass and volume will self-evidently be *a*) Minimizing spaceraft subsystem mass and *b*) Minimizing spaceraft subsystem volume. The attributes of this objective and corresponding QPMs are schematically given in Figure 4.6.

   To minimize the subsystems mass and volume, the measurable consequences will be the individual subsystems mass and volume respectively. We shall consider the mass

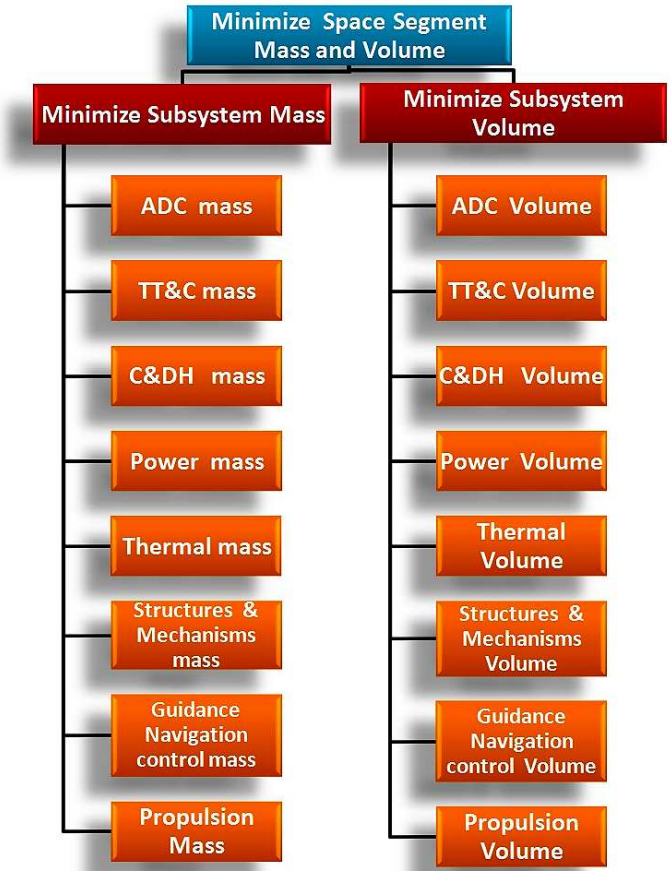

Figure 4.6: Minimize Space Segment Mass and Volume Objectives Hierarchy

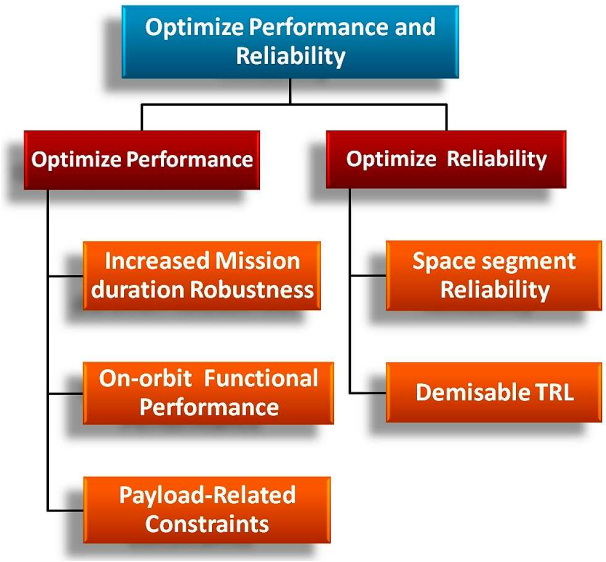

Figure 4.7: Optimize Performance and Reliability Objectives Hierarchy

and volume of the eight subsystems given in Figure 4.6. To minimize subsystems mass, the range of consequence will be from 0 to 1. For each individual subsystem, the lower value of consequence, 0, corresponds to the subsystem mass budget allocated by the project management as the highest possible acceptable, and the higher level of consequence, 1, will correspond to the ideal subsystem mass budget allocated by the project management. A similar procedure is followed in determining the range of consequence for the subsystems volume performance level.

4. **Optimize Performance and Reliability**
   The two attributes identified to optimize performance and reliability will self-evidently be *a*) Optimize performance and *b*) Optimize reliability. The attributes of this objective and corresponding QPMs are schematically given in Figure 4.7.

   Three measurable consequences identified as QPMs to optimize performance are; *Increased mission duration robustness*, *On-orbit functional performance* and *Payload-related constraints.*

- *Increased mission duration robustness*
  This QPM measures increased mission duration robustness introduced by designing for demise relative to a controlled reentry mission. Some missions, for example CGRO (see Section 1.2) have a zero-fault tolerance after initial controlled reentry subsystem failure. Consequently, this will lead to premature mission termination to guarantee a controlled reentry. However, a demisable spacecraft is relatively free of such constraints hence robustness to last the intended mission lifetime is vastly improved. The range of consequence will be from 0 to 1. The lower value of consequence, 0, corresponds to the guaranteed mission duration portion characterized by fault-free controlled reentry subsystem before the end of mission lifetime as determined by the project management. The higher level of consequence, 1, will correspond to the duration till the end of mission lifetime. A linear interpolation determines the values of consequence within the 0 - 1 range.

- *On-orbit functional performance*
  Re-designing the space segment for demise involves design alterations which may influence normal on-orbit functional performance relative to a non-demisable mission. For example, a demisable attitude and propulsion subsystem may affect the spacecraft slew rate, range, pointing accuracy, and settling time; a demisable power subsystem may affect energy storage capacity and efficiency; a demisable structure and mechanisms subsystem may affect the subsystem moment of inertia, bending strength, stiffness, and mechanisms reliability. The range of consequence will be from 0 to 1. The lower value of consequence, 0, corresponds to the lowest acceptable performance of the specific subsystem as determined by the project management. The higher level of consequence, 1, will correspond to the highest acceptable performance of the specific subsystem as determined by the project management. A linear interpolation determines the values of consequence within the 0 - 1 range.

- *Payload-related constraints*
  Constraints due the design of a demisable payload can influence mission performance in several ways. For example, to achieve demisability the size (mass and volume) of the payload may be reduced which may lower performance; an alternative lower performing demisable payload may be necessary, and so on. The range

of consequence will be from 0 to 1. The lower value of consequence, 0, corresponds to the unacceptable performance as determined by the project management. The higher level of consequence, 1, will correspond to the ideal acceptable performance as determined by the project management. A linear interpolation determines the values of consequence within the 0 - 1 range.

Two measurable consequences identified as QPMs to optimize reliability are; *Space segment reliability*, and *Demisable Technology Readiness Level.*

- *Space segment reliability*
  This is the computed space segment reliability *R(t)* whose range of consequence will be from 0 to 1. No performance level inference or interpolation is necessary since the *R(t)* values seamlessly confirm to the QPM metric criteria.

- *Demisable Technology Readiness Level*
  The NASA Technology Readiness Level (TRL) definition [34] is followed as shown in Figure 4.8. The range of consequence will be from 0 to 1. The lower value of consequence, 0, corresponds to TRL level 1. The higher level of consequence (1) will correspond to TRL level 9.

  A linear interpolation determines the values of consequence within the 0 - 1 range. To illustrate; Let

  $$C(0) = 1 \ \& \ C(1) = 9$$

  where:
  $C(n)$=Performace Level
  Applying Linear Interpolation:

  $$y = mx + c$$

  Then

  $$1 = 9x + c$$

  $$0 = x + c$$

  $$\Longrightarrow x = \frac{1}{8}, \ c = -\frac{1}{8}$$

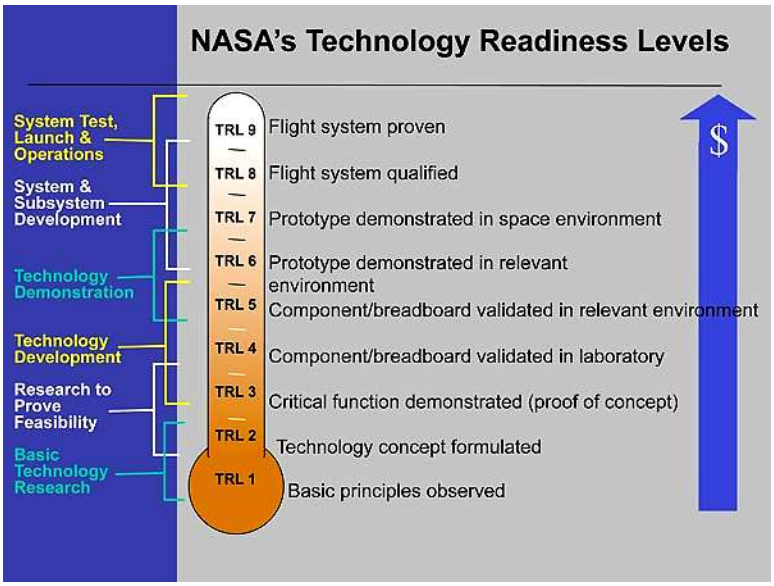

Figure 4.8: NASA Technology Readiness Levels. (Courtesy http://isse.arc.nasa.gov)

Hence Linear Interpolation equation becomes,

$$y = m\frac{1}{8} - \frac{1}{8}$$

Therefore, TRL=8 and TRL=3 will yield values of consequence equal to 0.875 and 0.25 respectively.

4.3 Chapter Summary

Chapter 4 introduced a deliberative decision making process - Analytical Deliberative Process (ADP), and applied it in making decisions to design for demise. We outlined the various Attributes, Quantitative Performance Measures (QPM) and demonstrated how to compute the level of consequences. Results from this process facilitate the decision to design for demise and bring together the the decision maker and other stakeholders. The ADP process can also be applied to post-mission disposal decision making process. This transpires before the choice for uncontrolled reentry is made. The steps detailed in this chapter imply a demisable uncontrolled reentry post-mission disposal option shown in Figure 4.2 has

been preferred over controlled reentry and non-demisable uncontrolled reentry with waivers disposal options.

Chapter 5

Design-for-Demise Trade-offs, Limitations and Case Application

After arriving at a decision to design-for-demise, we need to investigate the specific methods in re-designing a non-demisable component and make it demisable. This chapter will investigate these hardware DfD methods. Demisability trade-offs of parts from two perennial non-demisable subsystems: *a*) Propulsion subsystem, and *b*) Power Subsystem, will demonstrate the limitations and design trade-offs involved in DfD. Chapter 5 also describes the Design-for-Demise survivability analysis on a specific LEO mission. We shall consider the HETE-2 Mission launched in October 2000. The demisability analysis in DAS will encompass identifying the spacecraft parts to be analyzed by decomposing the spacecraft into parts; carrying out the analysis; and interpreting the results obtained. This chapter hence aims to apply the demisability analysis techniques assuming that a decision to design for demise has been reached using the ADP decision making procedure described in Section 4.2.

5.1 Design-for-Demise Trade-offs and Limitations

Re-designing the space segment to achieve demisability is likely to introduce inherent performance constraints and limitations. We shall give illustrative demonstrations on the limitations encountered when designing specific spacecraft parts for demise. The representative parts considered are perennial survivors from the propulsion and power subsystems. We shall also mention a designed to demise part of the attitude control subsystem. Firstly,

we describe some the specific methods employed in designing for demise.

5.1.1 Hardware Design-for-Demise Methods

The methods listed below are employed to transform a non-demisable spacecraft design to a demisable one. The methods are utilized in an iterative process involving reentry analysis software tools. Depending on the part under consideration, the methods can be used singly or in multiple combination.

- Different Material
  As outlined in Section 2.1, materials with a relatively lower melt temperature are more likely to ablate during reentry than those of relatively higher melt temperature. A part made of aluminum is more likely to demise than one made of titanium. Consequently re-designing a part by using a different material is one way to attain demisability. For instance a non-demisable stainless steel skirt for a tank can be replaced with one made of graphite epoxy which is demisable.

- Multiple material
  A part can be made to demise by replacing the non-demisable material with more than one different type of material that will result in demisability. For instance, titanium tanks can be replaced by Composite Overwrapped Pressure Vessels (COPV) [35] made from graphite composite and Al 6061 liner.

- Different shape
  Demisability is a function of the surface area to mass ratio. Changing the shape of an object to attain a relatively higher surface area to mass ratio can enhance demisability. For instance, a box or cylinder shape can be shown to be more likely to demise than a non-demisable flat panel of similar mass.

- Different size
  Changing the object dimensions (length, width, height or diameter), hence altering its mass to increase the object surface area to mass ratio will advance demisability likelihood. These changes are constrained within the mission requirements. For instance it can be demonstrated that the length or diameter of a propellant tank can be reduced to make it demisable.

- Change wall thickness
  Changing the wall thickness implies altering the mass of the object without necessarily changing the dimensions. This action has a similar effect of increasing the surface area-to-mass ratio. Consequently the object will be more likely to demise.

- Perforate material structure
  Putting holes in the object structure without compromising structural integrity acts to reduce the object mass. Therefore with a relatively decreased mass and increased surface area to mass ratio, the object is more likely to demise.

- Part structural location
  If a spacecraft part is located in close proximity to the spacecraft configuration structural boundary, it is exposed to the ablation environment relatively earlier than an inwardly located part. Consequently, its demise likelihood is elevated. On the contrary, if a part is structurally located towards the middle or inner sections of the of the spacecraft, it is exposed to the ablative environment after the parts around it demise or after a structural break-up occurs. Therefore, the relatively delayed exposure reduces the likelihood for demise. During the design for demise process, demisability can be enhanced by locating the relatively higher susceptible parts close to the structural center and the relatively less susceptible to demise parts towards the structural peripheries for earlier exposure.

5.1.2 Demisability Trade-offs and Limitations

Designing the space segment parts to demise can affect the performance and capability of the space system. Consequently in this section we examine some of the trade-offs undertaken, implications on performance and limitations of designing for demise. Demisable parts representing established perennial survivors (see Section 3.2.2) from the propulsion and power subsystems will be analyzed.

Propulsion subsystem

Propellant tanks perennially survive reentry because they are mostly made of non-demisable material such as titanium or stainless steel. Therefore, to make the tank demisable

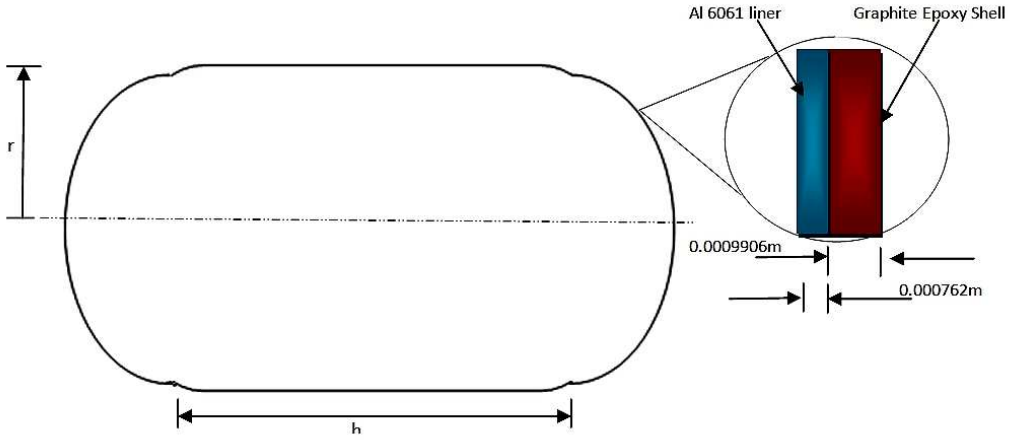

Figure 5.1: COPV tank shape and material mechanical properties.

a Composite Overwrapped Pressure Vessel (COPV) design is preferred. COPV is a pressure vessel with a composite shell fully or partially encapsulating a metallic liner. The liner serves as a fluid permeation barrier while the shell carries pressure and environmental loads [35].

We vary the capacity of a cylindrical COPV tank made of a graphite epoxy outer shell and an Aluminum 6061 liner. The capacity is varied by holding the outermost radius constant at 1 m, while varying the tank height. The tank has dome-shaped ends, a composite overwrap thickness of 0.39 inches (0.0009906 m) and an Al 6061 liner thickness of 0.03 inches (0.000762 m).

Composite overwrap and liner masses are determined from the density and volume of the materials for demisability analysis in DAS. We measure on-orbit performance by determining the amount of station keeping ΔV provided by a given tank configuration for a spacecraft with an initial mass of 3200 kg and hydrazine propellant occupying 96% of the tank. Finally, we determine the spacecraft mass fraction (ratio of final mass to initial mass) to provide an intuition into the spacecraft dry mass. The demisable tank performance is contrasted with that of a monolithic titanium non-demisable tank with a similar mass, a controlled reentry ΔV budget of 168 m/s and from an operational circular orbit of 405 km. Atmospheric reentry is taken to begin at an altitude of 120 km.

To determine the composite overwrap mass and Al 6061 liner mass, we use Equations 5.1

and 5.2 respectively.

$$m_s = \rho_s \pi \left[h \left(r_1^2 - r_2^2 \right) + \frac{4}{3} \left(r_1^3 - r_2^3 \right) \right] \tag{5.1}$$

And

$$m_l = \rho_l \pi \left[h \left(r_2^2 - r_3^2 \right) + \frac{4}{3} \left(r_2^3 - r_3^3 \right) \right] \tag{5.2}$$

Where:
m_s = composite overwrap mass, kg
m_l = Al 6061 mass, kg
$\rho_s = 1550.5\ kg/m^3$, graphite composite density
$\rho_l = 2707 kg/m^3$, Al 6061 density
h = tank height, m
r_i = tank radii, m. Here, distance from tank center to inner liner boundary corresponds to i=3, distance to Shell-liner junction (i=2), and distance to outer shell boundary (i=1).

Therefore, the tank mass is:

$$m_t = m_s + m_l \tag{5.3}$$

The mass of propellant contained in the tank (assuming 96% capacity) is calculated from the tank volume and hydrazine density in Equation 5.4.

$$m_p = 0.96 \rho_h \pi \left(h r_3^2 + \frac{4}{3} r_3^3 \right) \tag{5.4}$$

Where:
m_p = propellant mass, kg
$\rho_h = 980.94\ kg/m^3$, hydrazine density

Available on-orbit ΔV for a spacecraft with an initial mass of 3200 kg is computed by equation 5.5.

$$\Delta V = g I_{sp} ln \left(\frac{m_0}{m_f} \right) \tag{5.5}$$

The mass fraction (ratio of final mass to initial mass) is computed by Equation 5.6.

$$MF = \frac{m_f}{m_0} = e^{-\left(\frac{\Delta V}{gI_{sp}}\right)} \tag{5.6}$$

Where:
$g = 9.8\ m/s^2$, gravity acceleration
$I_{sp} = 220$ s, hydrazine specific impulse
m_0 = spacecraft initial mass, kg
m_f = spacecraft final mass, kg

Applying the above described formulas, data in Table 5.1 were obtained as the height is varied. The cylindrical tank has dome-shaped ends as shown in Figure 5.1.

Results of a similar analysis on a titanium monolithic tank for a controlled reentry LEO spacecraft are given in Table 5.2. Considering a functional orbit of 405 km, a controlled reentry ΔV budget of approximately 170 m/s is accounted for in the analysis.

To compare the performance of the COPV demisable tank and the non-demisable monolithic titanium tank, we plot the variations in Figure 5.2 and 5.3. DAS and ORSAT analysis show the monolithic titanium tank to be non-demisable while the COPV tank demises at an altitude of between 63 km and 72 km.

- **Propellant Mass Variation with Tank Mass**
  As the tank mass increases, the tank capacity also increases since the wall thickness is held constant and the height increases. Though the relationship between tank mass and propellant mass is linear for both tanks, the COPV tank yields a higher propellant mass for the same tank mass. This is because the COPV materials possess a lower density (graphite epoxy=1550.5 kg/m^3 and Al 6061= 2707kg/m^3) than the monolithic titanium tank of density 4400 kg/m^3. Material density is inversely related to the tank capacity for a fixed radius and thickness. The 'Propellant Mass Variation with Tank Height' plot complements the tank mass variation by showing how the tank height causes the propellant mass to vary. Therefore, the COPV tank has a more favorable

Table 5.1: COPV tank (Graphite epoxy/Al 6061) limitations and on-orbit performance.

COPV Tank (Graphite Epoxy shell /Al 6061 liner)							
	Shell	Liner	Tank Properties			On-orbit Performance	
Wall Thickness (m)	0.0009906	0.000762					
Material Density (kg/m^3)	1550.5	2707					
Outer Diameter (m)	1.016	1.0140188					
Inner Diameter (m)	1.0140188	1.0124948					
Cylinder Height (m)	Mass (kg)	Mass (kg)	Mass (kg)	Volume (m^3)	Propellant Mass (kg)	ΔV (m/s)	Mass Fraction
0.2	0.98	1.31	2.29	0.16	151.64	104.67	0.95
0.4	1.96	2.63	4.59	0.32	303.28	214.68	0.91
0.6	2.94	3.94	6.88	0.48	454.93	330.61	0.86
0.8	3.92	5.25	9.17	0.64	606.57	453.12	0.81
1.0	4.90	6.57	11.46	0.81	758.21	583.02	0.76
1.2	5.88	7.88	13.76	0.97	909.85	721.26	0.72
1.4	6.86	9.19	16.05	1.13	1061.49	868.96	0.67
1.6	7.84	10.51	18.34	1.29	1213.14	1027.53	0.62
1.8	8.82	11.82	20.63	1.45	1364.78	1198.70	0.57
2.0	9.80	13.13	22.93	1.61	1516.42	1384.64	0.53
2.2	10.77	14.45	25.22	1.77	1668.06	1588.14	0.48
2.4	11.75	15.76	27.51	1.93	1819.70	1812.88	0.43
2.6	12.73	17.07	29.81	2.09	1971.34	2063.79	0.38
2.8	13.71	18.39	32.10	2.25	2122.99	2347.79	0.34
3.0	14.69	19.70	34.39	2.42	2274.63	2674.97	0.29
3.2	15.67	21.01	36.68	2.58	2426.27	3060.84	0.24
3.4	16.65	22.33	38.98	2.74	2577.91	3531.15	0.19
3.6	17.63	23.64	41.27	2.90	2729.55	4133.54	0.15
3.8	18.61	24.95	43.56	3.06	2881.20	4972.44	0.10
4.0	19.59	26.26	45.86	3.22	3032.84	6364.38	0.05
4.2	20.57	27.58	48.15	3.38	3184.48	11488.77	0.00
4.4	21.55	28.89	50.44	3.54	3336.12		
4.6	22.53	30.20	52.73	3.70	3487.76		
4.8	23.51	31.52	55.03	3.86	3639.41		
5.0	24.49	32.83	57.32	4.03	3791.05		
5.2	25.47	34.14	59.61	4.19	3942.69		
5.4	26.45	35.46	61.90	4.35	4094.33		
5.6	27.43	36.77	64.20	4.51	4245.97		
5.8	28.41	38.08	66.49	4.67	4397.61		
6.0	29.39	39.40	68.78	4.83	4549.26		
6.2	30.37	40.71	71.08	4.99	4700.90		
6.4	31.35	42.02	73.37	5.15	4852.54		
6.6	32.32	43.34	75.66	5.31	5004.18		
6.8	33.30	44.65	77.95	5.48	5155.82		

Table 5.2: Monolithic titanium tank limitations and effect on performance

Monolithic Titanium Tank					
	Tank Mechanical Properties			On-Orbit Performance	
	Tank Thickness = 0.006 m		Outer Diameter = 1 m		
	Ti Density = 4400 kg/m^3		Inner Diameter = 0.994 m		
Tank Mass (Kg)	Tank Height (m)	Volume (m^3)	Propellant Mass (kg)	ΔV	Mass Fraction
2.29	0.05	0.04	40.00	-	0.99
4.59	0.11	0.09	80.53	-	0.97
6.88	0.17	0.13	121.05	-	0.96
9.17	0.22	0.17	161.93	-	0.95
11.46	0.28	0.21	202.46	-	0.94
13.76	0.33	0.26	242.98	1.63	0.92
16.05	0.39	0.30	283.51	31.38	0.91
18.34	0.44	0.34	324.20	61.67	0.90
20.63	0.50	0.39	364.56	92.14	0.89
22.93	0.55	0.43	405.08	123.18	0.87
25.22	0.61	0.47	445.60	154.67	0.86
27.51	0.67	0.52	486.13	186.62	0.85
29.81	0.72	0.56	526.65	219.06	0.84
32.10	0.78	0.60	567.18	251.99	0.82
34.39	0.83	0.65	607.70	285.44	0.81
36.68	0.89	0.69	648.23	319.41	0.80
38.98	0.94	0.73	688.75	353.92	0.78
41.27	1.00	0.77	729.28	389.00	0.77
43.56	1.05	0.82	769.80	424.65	0.76
45.86	1.11	0.86	810.33	460.91	0.75
48.15	1.16	0.90	850.85	497.78	0.73
50.44	1.22	0.95	891.37	535.30	0.72
52.73	1.28	0.99	931.90	573.48	0.71
55.03	1.33	1.03	972.42	612.35	0.70
57.32	1.39	1.08	1012.95	651.94	0.68
59.61	1.44	1.12	1053.47	692.26	0.67
61.90	1.50	1.16	1094.00	733.35	0.66
64.20	1.55	1.20	1134.52	775.24	0.65
66.49	1.61	1.25	1175.05	817.96	0.63
68.78	1.66	1.29	1215.57	861.55	0.62
71.08	1.72	1.33	1256.26	906.22	0.61

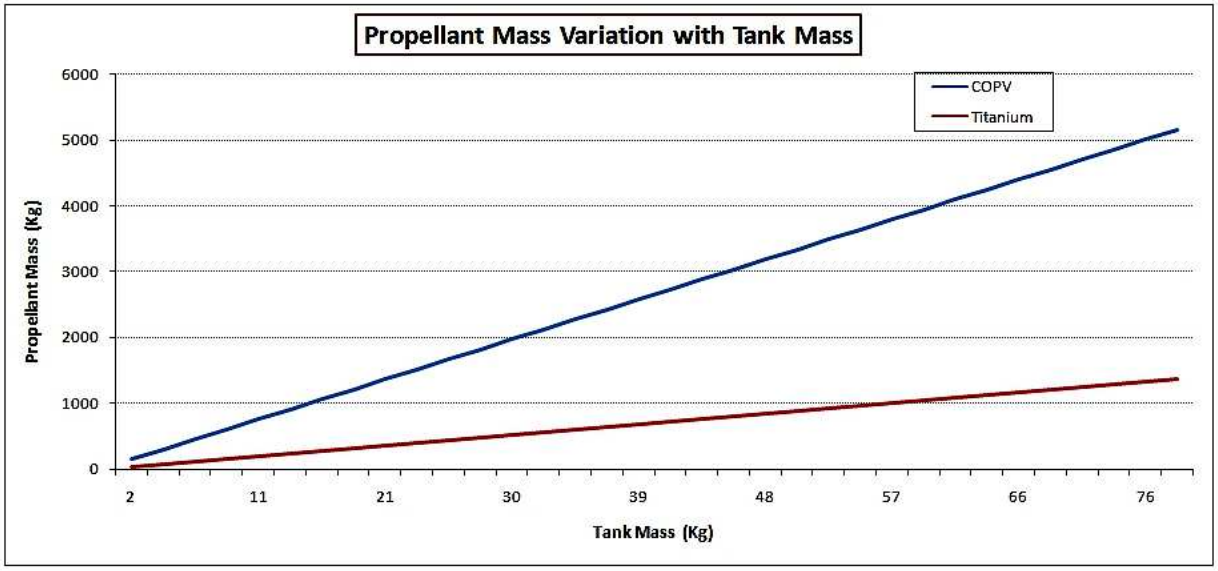

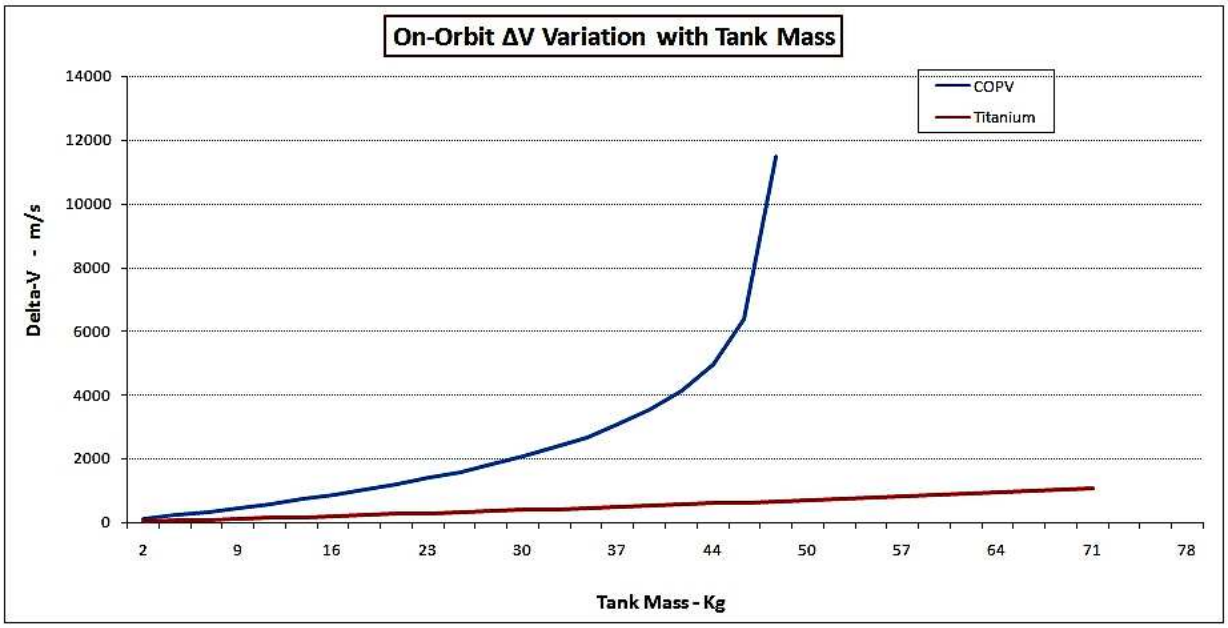

Figure 5.2: Demisable (COPV) and non-demisable (titanium) tank performance comparison

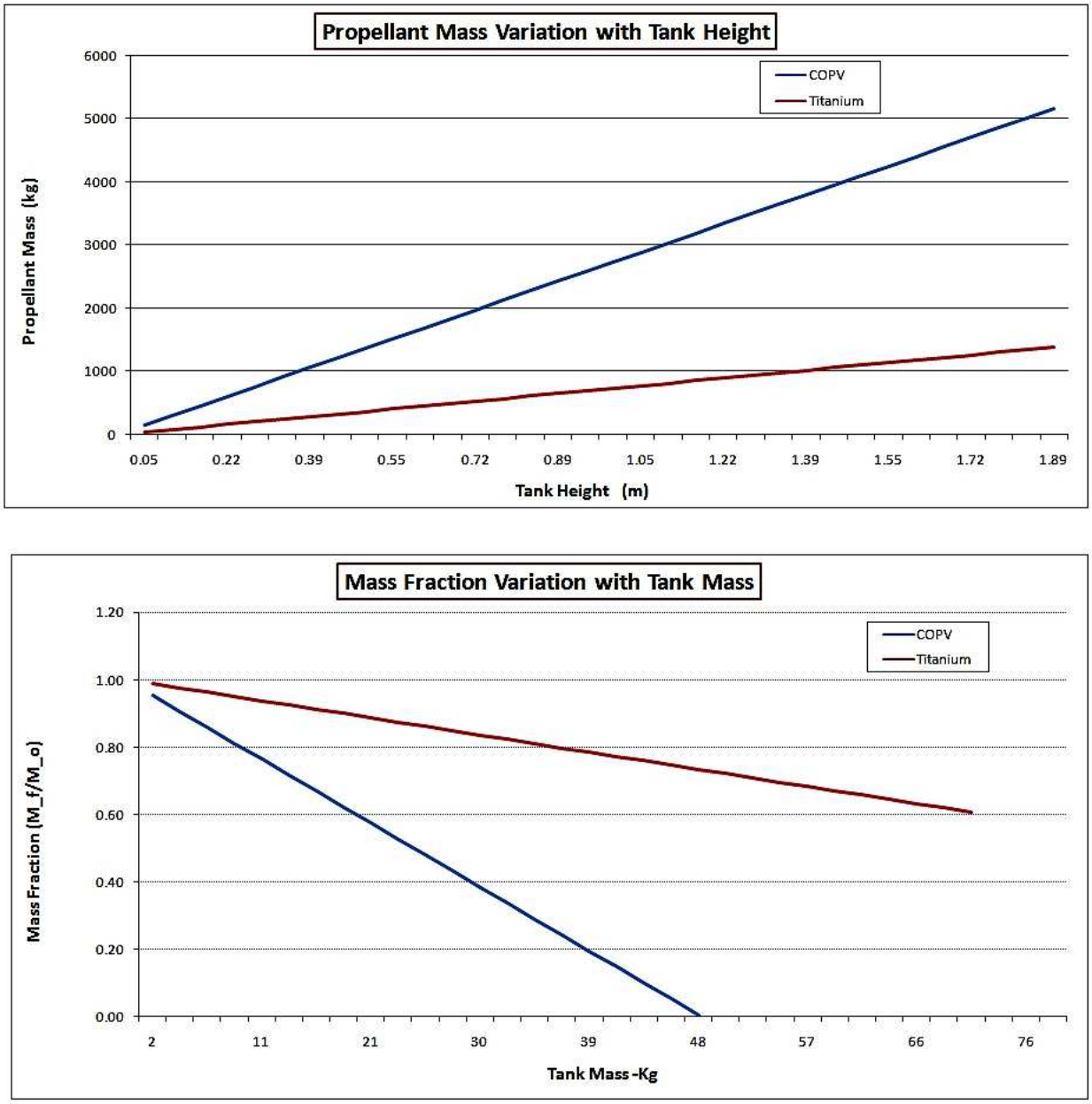

Figure 5.3: Additional Demisable (COPV) and non-demisable (titanium) tank performance comparison

performance because it is capable of holding a higher fuel mass than the titanium tank for a given tank mass.

- **On-Orbit ΔV Variation with Tank Mass**
  Since a demisable COPV tank holds more propellant than a monolithic titanium tank of the same mass, the COPV tank has a better on-orbit ΔV performance for the 3200 kg spacecraft case considered. Though the trend seems to climb drastically as the tank mass increases, we restrict ourselves to a practical mass fraction range range of higher than 0.6 (i.e. 60% dry mass and higher) which corresponds to a ΔV value of less than 1030 m/s. Scrutinizing the tank performances in the restricted mass fraction region, the demisable COPV tank is more favorable than the non-demisable titanium tank because of the associated higher on-orbit ΔV figure.

- **Mass Fraction Variation with Tank Mass**
  The COPV tank yields a lower mass fraction than a monolithic titanium tank for the same tank mass on the 3200 kg spacecraft. This is because for a similar mass, the demisable COPV tank holds more propellant than the non-demisable monolithic titanium tank. Consequently, the dry mass of the 3200 kg spacecraft with a COPV tank will be lower compared to the same spacecraft with a non-demisable monolithic titanium tank of a similar mass. Further, for the same mass fraction (e.g. 0.8), the demisable COPV tank has a mass of about $\frac{1}{3}$ the mass of the titanium tank. On-orbit performance is hence favorable for the demisable tank, constrained only by the mission mass fraction requirement.

Power subsystem

From the hierarchical decomposition of the power subsystem in section 3.2.1, the power storage assembly is more likely to survive reentry compared to the other power subsystem assemblies. We hence consider the battery as the representative part for analysis here.

We again consider a 3200 kg spacecraft with a power budget of 1.5 kW. To conduct the demisability trade-offs and limitations in sufficing the 1.5 kW power budget, we take into account a small sample of flight-proven, off-the-shelf, commercially available batteries. Typically NiMH cells are non-demisable pressure vessels with a stainless steel casings. On

Table 5.3: *Quallion* and *Saft* Li-ion cell mechanical properties.

Manufacturer	Brand Name	Diameter/width (m)	Length(m)	Height (m)	Weight (kg)	Weight Energy density (Wh/kg)	Casing Thickness (m)
Quallion	18650 SA	0.0181		0.0648	0.0434	102	0.0004
	18650 W	0.0181		0.0648	0.046	116	0.0004
	18650 Y	0.0181		0.0648	0.043	163	0.0004
	18650 F	0.0181		0.0648	0.047	196	0.0004
	QL0032A	0.0074	0.05	0.12	0.097	120	0.0004
	QL0045A	0.0071	0.05	0.105	0.078	120	0.0004
	QL015KA	0.0380	0.0545	0.0883	0.38	142	0.0004
	QL075KA	0.0562	0.0809	0.1737	1.82	148	0.0008
Saft	LSH 20HTS	0.0334		0.0616	0.1	149	0.0004
	LSH 20	0.0334		0.0616	0.1	149	0.0004
	LSH 14	0.0260		0.0504	0.051	149	0.0004
	LSH 26180	0.0262		0.0186	0.024	149	0.0004
	VES 100	0.0530		0.185	0.81	118	0.0005
	VES 140	0.0530		0.25	1.13	126	0.0008
	VES 180	0.0540		0.251	1.11	175	0.0008
	VL 48 E	0.0540		0.245	1.15	150	0.0008
	VL 45 E	0.0543		0.222	1.07	149	0.0008
	VL 52 E	0.0540		0.208	1	185	0.0008
	8S3P	0.0950	0.17	0.22	4.5	165	0.0008
	8S LD25P	0.0760	0.11	0.21	2.2	165	0.001

the contrary, Li-ion cells are characterized by low pressure operation with an aluminum casing and are hence demisable.

We take a sample of Li-ion cells from two manufacturers; *Quallion llc* of USA and *Saft* of France. The brand names with corresponding mechanical characteristics are given in Table 5.3.

Using the cell gravimetric energy density (Wh/kg), and an orbit time when the battery supplies power, we compute the mass of cells required to meet the 1.5 kWh energy requirement in Equation 5.7. We let the battery supply power for half the orbit duration i.e. 45 minutes. Then, add a conservative allowance of 15 minutes to this time. The estimated orbit time when the battery supplies power is hence taken to be 1 hour. Corresponding cell quantity is computed as shown in Equation 5.8.

$$m_{1.5kW} = \frac{power\ budget\ (W) \times time\ (h)}{gravimetric\ energy\ density\ (Wh/kg)} \tag{5.7}$$

$$N = \frac{m_{1.5kW}}{m_{cell}} \tag{5.8}$$

$$m_c \approx \rho_c \pi \left[l \left(r_1^2 - r_2^2 \right) \right] \tag{5.9}$$

Where:

$m_{1.5kW}$ = total battery mass for a 1.5 kW power budget, kg

$time = 1$ hour, estimated orbit time when the battery supplies power
m_{cell} = individual cell mass, kg
N = quantity of cells required for a 1.5 kW power battery
m_c = casing mass, kg
ρ_c = casing material density kg/m^3
l = cell height, m
r_i = cell radii, m. Here, distance from cell center to the inside of cell casing corresponds to i=2, and distance to the outside of cell casing corresponds to i=1.

In carrying out reentry analysis, we examine the cell casing and assume that the enclosed chemical reactants are demisable. To determine the casing thickness, we let the cell casing thickness to vary from a conservative value of 0.4 mm to 1.0 mm based on measurements conducted on a sample cell in Section 5.3.1. Next, we compute the casing mass from the material density (Al density = 2700 kg/m^3, Stainless Steel density = 7800 kg/m^3), and volume as shown in Equation 5.9. Finally the demisabilty analysis in DAS is carried out by clustering the individual cells into groups of 133 or fewer contained in a demisable enclosure made of aluminum or graphite epoxy. A sample DAS entry is shown in Figure 5.4.

The above Li-ion battery characteristics are contrasted from those of a different battery by considering cells with similar masses as the listed brands, but with a stainless steel casing instead of an aluminum casing. An analysis similar to the one carried out for the aluminum case is undertaken. The resulting data is given in Table 5.4.

Subsequent trends are plotted in Figure 5.5 and 5.6

Figure 5.5(a) shows the variation of mass among the cell brands needed to meet the 1.5 kW power budget. The cell with the highest gravimetric energy density (Wh/kg) yields the lowest mass. For instance, from a design point of view, the *Quallion 18650F* brand is favorable due to its lowest mass of 7.65 kg for a 1.5 kW mass budget. In Figure 5.5(b), we consider cells with the same mass as the obtained brand names. Assuming a similar case thickness, we plot the casing mass for an Aluminum case and stainless Steel case for a given cell mass. For the same thickness, the stainless steel case has a bigger mass than the

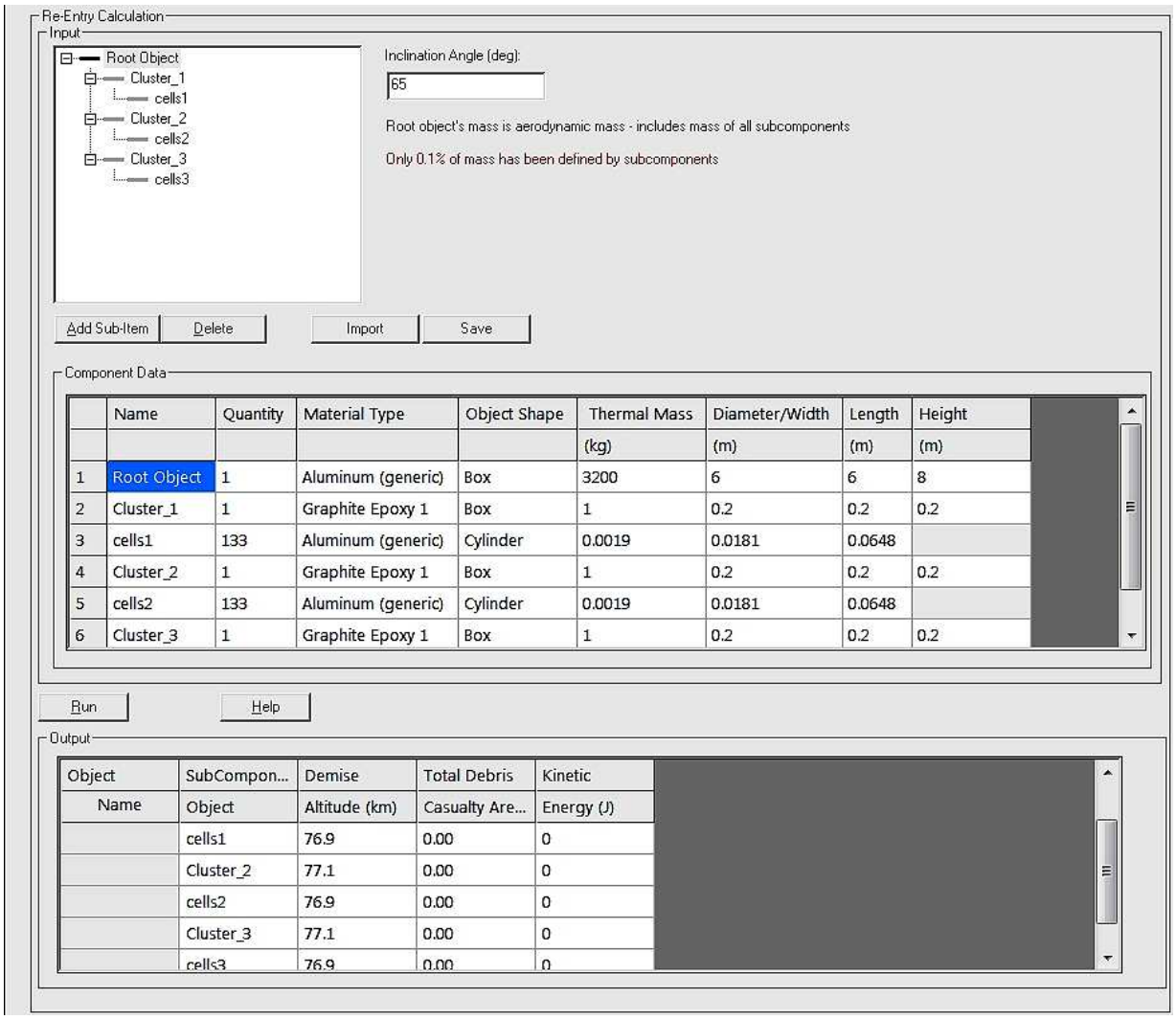

	Name	Quantity	Material Type	Object Shape	Thermal Mass (kg)	Diameter/Width (m)	Length (m)	Height (m)
1	Root Object	1	Aluminum (generic)	Box	3200	6	6	8
2	Cluster_1	1	Graphite Epoxy 1	Box	1	0.2	0.2	0.2
3	cells1	133	Aluminum (generic)	Cylinder	0.0019	0.0181	0.0648	
4	Cluster_2	1	Graphite Epoxy 1	Box	1	0.2	0.2	0.2
5	cells2	133	Aluminum (generic)	Cylinder	0.0019	0.0181	0.0648	
6	Cluster_3	1	Graphite Epoxy 1	Box	1	0.2	0.2	0.2

Object Name	SubCompon... Object	Demise Altitude (km)	Total Debris Casualty Are...	Kinetic Energy (J)
	cells1	76.9	0.00	0
	Cluster_2	77.1	0.00	0
	cells2	76.9	0.00	0
	Cluster_3	77.1	0.00	0
	cells3	76.9	0.00	0

Figure 5.4: Battery demisability analysis in DAS

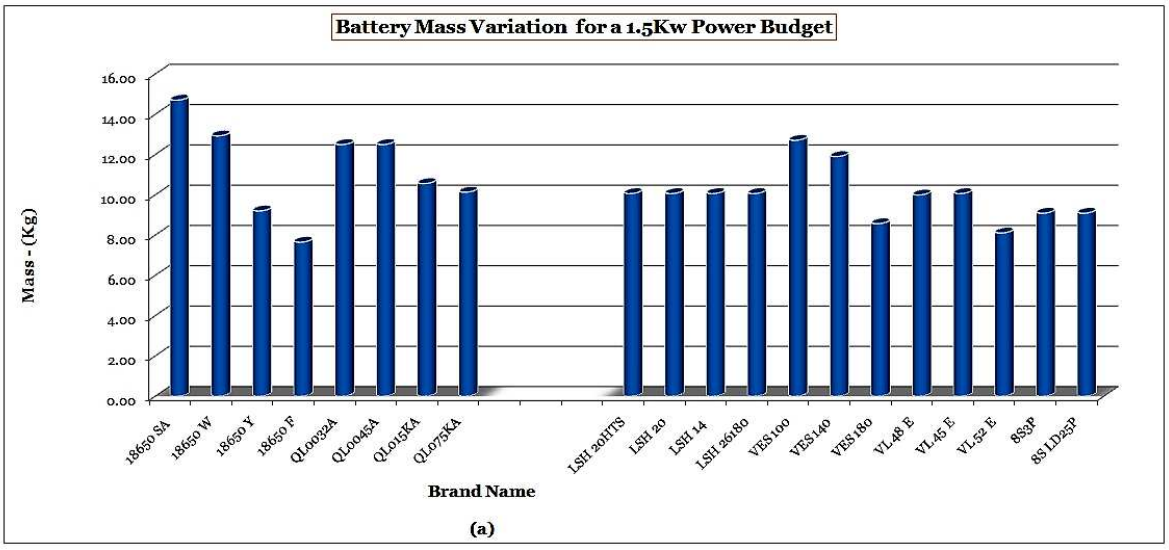

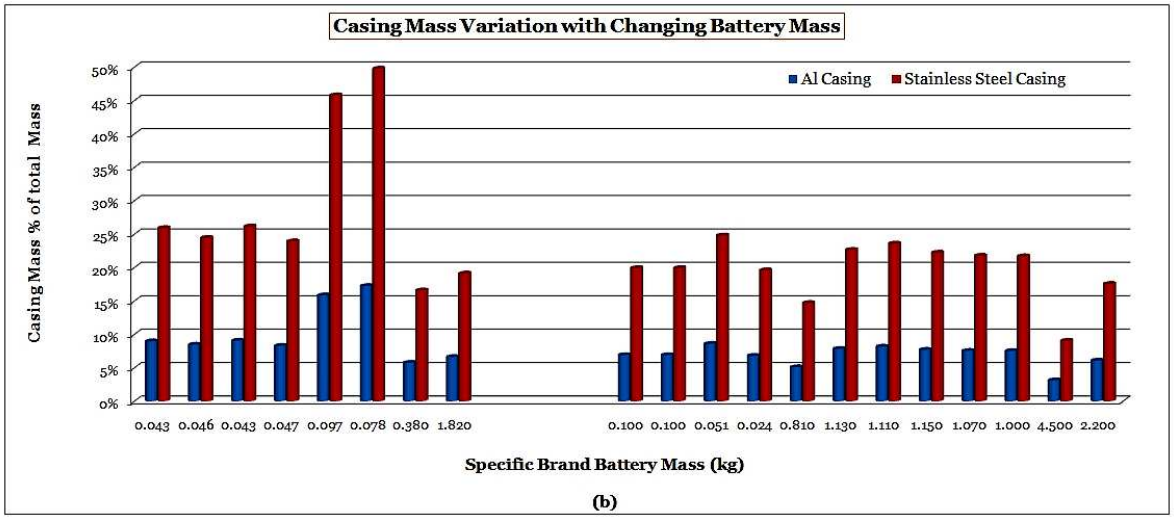

Figure 5.5: Demisable and non-demisable battery characteristics for a 1.5 kW power budget

Table 5.4: Demisable and non-demisable battery characteristics.

Manufacturer	Brand Name	Weight for 1.5kW(kg)	Quantity for 1.5kWh	Li-ion Casing mass (kg)	Li-ion demise alt (km)	SS Casing mass (kg)	Remarks
Quallion	18650 SA	14.71	338.85	0.003892	72.0	0.0112422	3 clusters of 113 cells grouped together
	18650 W	12.93	281.11	0.003892	72.0	0.0112422	3 clusters of 94 cells grouped together
	18650 Y	9.20	214.01	0.003892	72.0	0.0112422	3 clustersof 72 cells grouped together
	18650 F	7.65	162.83	0.003892	72.0	0.0112422	3 clusters of 55 cells grouped together
	QL0032A	12.50	128.87	0.015372	72.6	0.0444083	3 clusters of 43 cells grouped together
	QL0045A	12.50	160.26	0.013438	72.7	0.0388219	3 clusters of 54 cells grouped together
	QL015KA	10.56	27.80	0.021805	72.3	0.0629912	1 cluster of 28 cells grouped together
	QL075KA	10.14	5.57	0.120382	71.4	0.3477693	1 cluster of 6 cells grouped together
Saft	LSH 20HTS	10.07	100.67	0.006897	72.2	0.0199250	2 clusters of 52 cells grouped together
	LSH 20	10.07	100.67	0.006897	72.2	0.0199250	2 clusters of 52 cells grouped together
	LSH 14	10.07	197.39	0.004378	69.8	0.0126466	3 clusters of 66 cells grouped together
	LSH 26180	10.07	419.46	0.001628	70.4	0.0047037	4 clusters of 104 cells grouped together
	VES 100	12.71	15.69	0.041192	71.7	0.1189996	2 clusters of 8 cells grouped together
	VES 140	11.90	10.54	0.088555	71.2	0.2558262	2 clusters of 5 cells grouped together
	VES 180	8.57	7.72	0.090613	71.0	0.2617700	2 clusters of 4 cells grouped together
	VL 48 E	10.00	8.70	0.088447	71.2	0.2555125	2 clusters of 5 cells grouped together
	VL 45 E	10.07	9.41	0.080595	71.1	0.2328312	2 clusters of 5 cells grouped together
	VL 52 E	8.11	8.11	0.075089	71.0	0.2169249	2 clusters of 4 cells grouped together
	8S3P	9.09	2.02	0.140630	71.5	0.4062637	1 cluster of 2 cells grouped together
	8S LD25P	9.09	4.13	0.133596	71.1	0.3859447	2 cluster of 2 cells grouped together

aluminum case found in Li-ion battery.

In Figure 5.6, all the Li-ion brands needed for a 1.5 kW power budget demise. The *Quallion* brands demise at an altitude of between 71.4 km and 72.7 km while the *Saft* brands demise at an altitude of between 69.8 km and 72.2 km. All the Stainless Steel casing cases were non-demisable.

In Tables 5.1 and 5.2, representing subsystem trade-offs and limitations, the yellow highlighted band represents values applicable to the GPM mission core spacecraft. Moreover, the chosen spacecraft mass of 3200 kg is based on the mass of the GPM mission core spacecraft. The light green highlighted band represents the design limit for example where the entire spacecraft would have to be propellant giving a Mass Fraction of zero. We chose to vary the tank height rather than the diameter, because the diameter is limited by the fixed launcher diameter which is less flexible. Consequently, a conservative diameter value of 1 m was preferred.

It is also worth mentioning the demisable Reaction Wheel Assembly (RWA) developed at NASA Goddard Flight Center [36]. Goddard's RWA design achieves demisability by combining favorable materials, specific parts design and layout. It has an aluminum flywheel and a stator containing very little iron. This effort is geared towards the GPM mission.

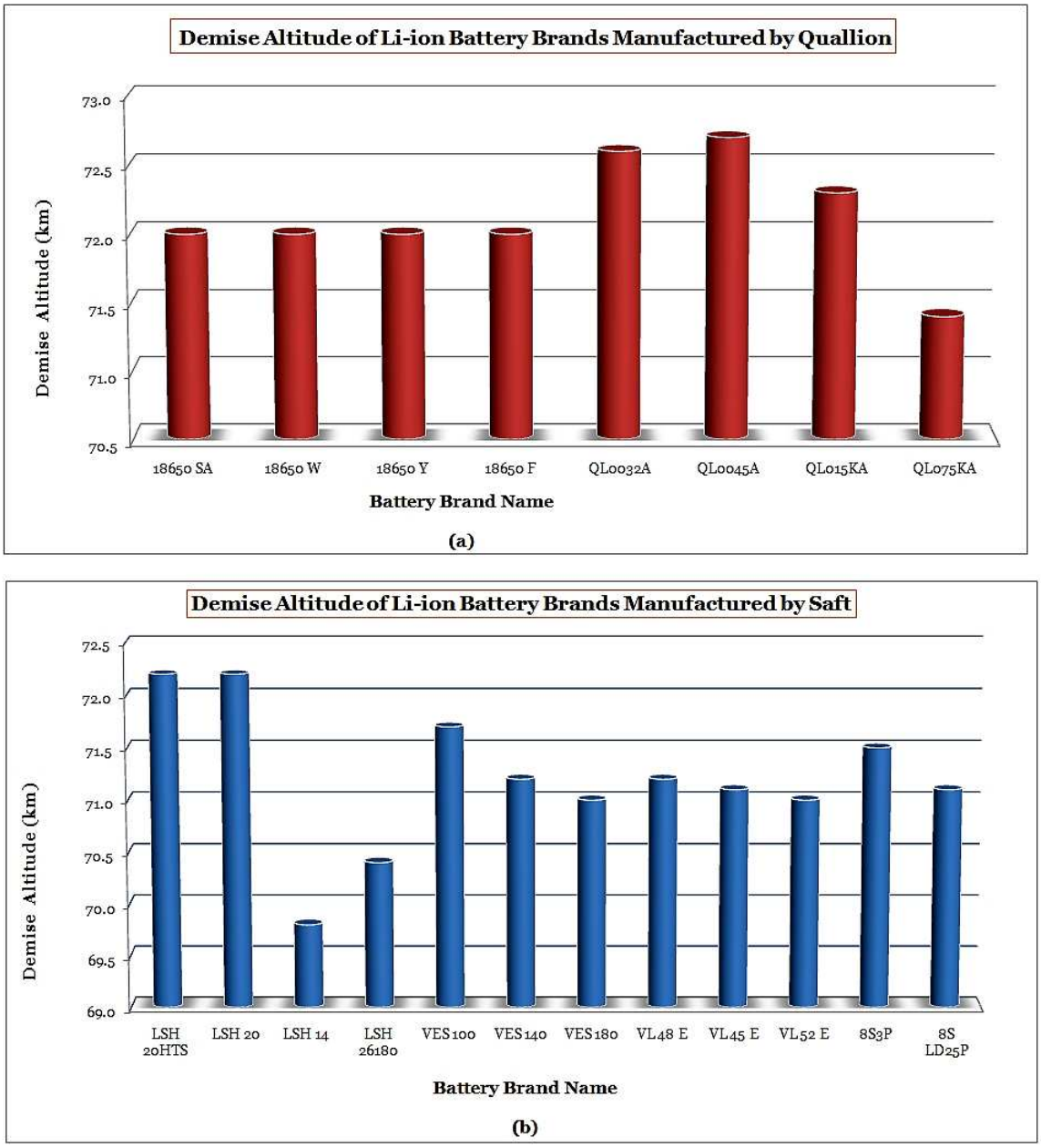

Figure 5.6: Demise altitudes for Li-ion battery for a 1.5kW power budget

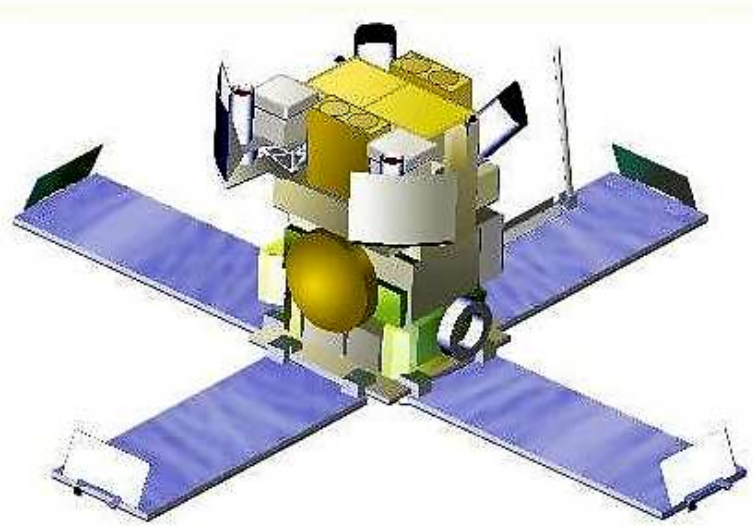

Figure 5.7: HETE-2 spacecraft. (Courtesy: MKI)

5.2 Case Study: HETE-2 Mission

The High Energy Transient Explorer (HETE) is an international collaboration mission to detect and localize gamma-ray bursts. It is led by the Center for Space Research at MIT. The other partners in the program include RIKEN, LANL, CESR, University of Chicago, University of California, Berkeley, University of California, Santa Cruz, CNES, Sup'Aero, CNR, INPE, and TIFR [37]. The coordinates of gamma-ray bursts detected are promptly relayed to a network of interested ground observers.

The HETE-2 is a small spacecraft shown in Figure 5.7, constructed with specifications and performances described in Table 5.5.

The spacecraft structure is chiefly made up of two parts; the bottom half (closest to the solar panels), consisting of mostly spacecraft hardware and the upper half (furthest from the solar panels) , where the science instruments reside. The bottom half has a marmon ring connected to a baseplate that supports the power and electronics boxes. Attitude is sensed by a combination of 2 magnetometers, a set of 12 coarse, medium, and fine sun sensors, and an optical camera system. Spacecraft attitude control is achieved via 3 orthogonal torque coils and a momentum wheel, which nominally spins at roughly 1800 RPM. Communication is conducted using an S-band radio, 5 dual patch transmit-receive S-band antennas, a VHF

Table 5.5: HETE-2 spacecraft and mission specifications. (Courtesy: MKI)

Item	**Specification**
Mass	124 kg
Envelope	Fits within cylinder 89 cm × 66 cm diameter
Desired orbit	625 km circular, $0 - 2^0$ inclination
Operating life	18 months, nothing to preclude 2+ years
Attitude	Sun pointing, Momentum bias, Attitude controlled to $\pm 2^0$
Data processing	4 T805 transputers, 8 DSP56001, $\sim$ 100 MIPS
Data Buffering	96 MB of EDAC mass memory
Down link	250 Kbs data rate, overall bit error rate $< 2 \times 10^{-8}$
Up link	31.25 Kbs data rate, overall bit error rate $< 10^{-8}$
Radio Frequencies	S-band uplink/downlink, VHF down link

transmitter and a VHF antenna. Power is delivered by 4 solar panels, and 6 battery packs. Four 4 processor boards handle the C&DH. Refer to **Appendix A** for the complete list of HETE-2 spacecraft parts.

5.3 HETE-2 DAS Survivability Analysis

As described in Section 3.2 we precede DAS survivability analysis by identifying spacecraft parts that are unlikely to demise based on their mass and material type. We identify individual parts of HETE-2 to be analyzed in DAS from the list given in Appendix A. Due to non-homogeneity of individual parts' material composition, the analyzed thermal mass is less than the actual mass of the entire part in most cases. For each non-homogeneous part, the thermal mass of the portion likely to survive reentry is taken to be dominant over the thermal mass of the portion likely to demise. For instance, if a sun sensor is made up of a copper alloy and plastic materials, the thermal mass of the copper alloy portion is taken to be dominant and hence considered for demisability analysis.

5.3.1 Thermal Mass Computation

We compile a list of possible non-demisable parts from the complete spacecraft parts list (see Appendix A) plus their corresponding physical properties - thermal mass, material type,

shape, dimensions and quantity used.

Specifically, we need to compute the thermal mass for the HETE-2 spacecraft power subsystem because the thermal mass differs most from the actual mass in this subsystem. The power subsystem hardware is composed of:

- 4 solar panels, made of honeycomb aluminum with silicon substrate, each supplying 42W
- Power control box
- 6 battery packs, each made up of a string of 23 1.2V NiCd cells, and each cell with 1.5 A-hrs capacity

Solar panels characteristically break up and demise during reentry. Therefore, we can safely assume here they will demise and exempt them from DAS demisability analysis. The power control box actual mass is also treated as the thermal mass. However, the thermal mass of the NiCd cells must be computed, because it differs significantly from the actual mass. Three twin battery packs consisting of 43 cells each are used to give a total of 138 cells in the HETE-2 spacecraft. Each cell has a mass of 52 g, diameter of 22 mm, and a height of 4.2 cm.

To obtain the thermal mass of an individual cell , we, *i)* dissect the individual cell; *ii)* obtain the stainless steel casing and discard the electrolyte compounds (assumed to be demisable); *iii)* flatten and measure the stainless steel casing thickness; and *iv)* use Equation 4.10 to obtain the casing mass.

This procedure yields the stainless steel casing thickness, 't' as;

$$t = 0.4mm$$

also,

$$t = (r_1 - r_2)$$

And,

$$casing\ mass \approx 15g$$

Table 5.6: HETE-2 parts for demisability analysis in DAS

HETE-2 PARTS For DEMISABILITY ANALYSIS									
Subsystem	**Subassembly**	**Part**	**Quantity**	**Material**	**Shape**	**Width/Dia (m)**	**Height (m)**	**Length (m)**	**Thermal Mass (kg)**
Structure		Marmon ring	1	Al	Flat plate	0.45	0.03		1.28
	Electronics Boxes	Command EB	1	Al	Box	0.2	0.2	0.2	12.12
		SXC EB	1	Al	Box	0.09	0.11	0.37	1.86
		Opt Camera EB	1	Al	Box	0.09	0.11	0.37	1.84
		Interface plate	1	Al	Box	0.02	0.45	0.45	6.44
		Harness	1	Cu	Cylinder	0.01	2		4.84
ADCS	Attitude Sensors	Magnetometer	2	Cu	Box	0.03	0.04	0.1	0.15
		Sun Sensor_1	1	Cu	Box	0.05	0.058	0.07	0.12
		Sun Sensor_2	1	Cu	Box	0.048	0.06	0.067	0.0159
		Sun Sensors_3	2	Cu	Box	0.004	0.19	0.18	0.52
		Sun Sensors_4	2	Cu	Box	0.41	0.004	0.18	1.02
		Sun Sensors_5	2	Cu	Box	0.005	0.2	0.17	0.69
		Aspect Opt camera	2	Cu	Cylinder	0.14	0.14		0.95
	Active Control	Torque Coil1	1	Cu	Cylinder	0.16	0.04		2.56
		Torque Coil2	1	Cu	Cylinder	0.23	0.02		1.63
		Torque Coil3	1	Cu	Cylinder	0.32	0.03		1.63
		Momentum Wheel	1	Cu	Cylinder	0.27	0.05		3.16
Communication	Transponder	S-band Transceiver	1	Cu	Box	0.3	0.3	0.3	4.73
		VHF Transmitter	1	Cu	Box	0.0015	0.035	0.048	0.065
	Antenna	S-band antennas	6	Al	Box	0.006	0.13	0.21	1.17
		GPS Antenna	1	Al	Cylinder	0.1	0.0038		1.02
		VHF antenna	1	Al	Box	0.0013	0.01	0.53	0.0091
Power		Power Control Box	1	Al	Box	0.1	0.13	0.37	4.39
	Battery Pack		3	Al	Box	0.14	0.06	0.275	1.85
		Cells	138	SS	Cylinder	0.022	0.042		0.015
Payload	FREGATE		4	Cu	Cylinder	0.1	0.2		2.18
		Fregate Electronics	1	Cu	Box	0.13	0.12	0.3	4.5
	WXM		1	Cu	Box	0.17	0.19	0.38	9.85
	SXC		2	Al	Box	0.1	0.1	1.75	2.36
	Boresight Camera		2	Al	Cylinder	0.07	0.14		0.65

This data is collected as shown in Table 5.2 which neglects thermal masses from parts that are known to have a propensity to demise. Data in Table 5.2 is inserted into DAS Reentry Survivability module to determine the *critical* (non-demisable) parts.

5.3.2 Results

HETE-2 is a relatively small spacecraft compared to the GPM mission core spacecraft. Nevertheless, the demisability techniques demonstrated here can seamlessly be extended to other spacecraft including GPM mission core spacecraft. The demisability analysis yield the Demise Altitude, Total Debris Casualty Area and the impacting KE of each non-demisable

Table 5.7: HETE-2 non-demisable parts DCA and KE.

Part Name	**Thermal Mass-kg**	**DCA-m^2**	**KE-Joules**
Marmon ring	1.3	0.72	175
Interface plate	6.44	0.86	4262
Harness	4.84	1.72	517
Sun Sensor3	0.52	1.07	171
S-band Transceiver	4.73	0.81	1873
Total	17.83	5.18	6998

part.

DAS analysis show that 14% of the HETE-2 spacecraft mass is likely to be non-demisable. The non-demisable parts concerned are given in Table 5.3. As detailed in Section 3.1.1, DAS is a relatively moderate fidelity tool with inherent conservatism. Therefore, the non-demisable parts making up 14% of the spacecraft mass need to be analyzed further in higher fidelity tools such as ORSAT to obtain a more accurate demisability prediction. The parts determined to be non-demisable by ORSAT (or other higher fidelity tools) can then be subjected to the hardware Design-for-Demise methods described in Section 4.3.1 to make them demisable. The marmon ring, interface plate and harness can be re-designed to demise by using a different material, size or by perforating them. If higher fidelity analysis still show the sun sensor and transceiver to be non-demisable, other demisable models could be explored.

Moreover, the analyzed HETE-2 parts demise at different altitudes due to their shape, size and type of material. This variation is given in Figure 5.8. Though momentum wheels are known perenial survivors, the HETE-2 mometum wheel will most likely demise. Despite information on the exact material composition of the 3.16 kg momemetun wheel not being available, we analyzed the momentum wheel using two different materials. In the first case, copper alloy was used as the type of material making the momentum wheel which demised at an altitude of 65.8 km. Stainless steel (with a higher melt temperature) demises at an altitude of 57.5 km. Consequently, the demisability of the two considered extreme cases of momentum wheel potential materials implies that the HETE-2 momentum wheel is most

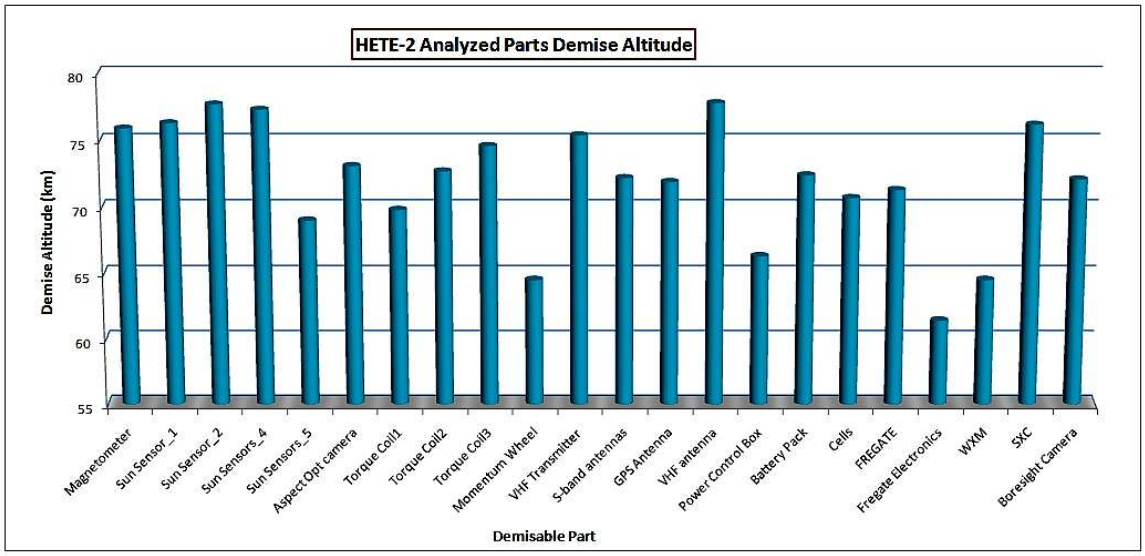

Figure 5.8: HETE-2 parts demise altitudes.

likely to demise too.

DAS predicts the uncontrolled atmospheric reentry of HETE-2 mission to have a human casualty risk of 1:29200 (0.00003425). *Requirement 4.7-1* of the the NASA Technical Standard 8719.14 - *Process for Limiting Orbital Debris*[1] stipulates that; for any object with an impacting kinetic energy in excess of 15 Joules for uncontrolled reentry, the risk of human casualty from surviving debris shall not exceed 0.0001 (1:10,000). Consequently, HETE-2 meets the NASA requirement for limiting the risk of human casualty despite having non-demisable parts. Re-designing spacecraft components to achieve demisability will not be necessary for this particular mission. However, designing for demise is described to illustrate the steps required in case a mission is fails to meet the human casualty risk requirement.

5.4 Chapter Summary

This chapter described the methods employed in transforming non-demisable spacecraft parts into demisable. These methods can be used in combination or individually to achieve demisability. Trade-off analysis of two parts from the representative subsystems of propellant tank (propulsion subsystem) and batteries (power subsystem) is done and the on-orbit per-

formance limitation investigated. Not only is the COPV tank demisable, it is also favorable due to its relatively lower mass for the same capacity as a monolithic titanium tank.

Chapter 5 applied the Design-for-Demise reentry survivability on an actual mission case. The HETE-2 spacecraft was selected as a case study because information regarding the spacecraft parts was readily available to the author. We segregated the potential non-demisable parts for DAS reentry demisability based on known perennial survivors, thermal mass, size and material type. This chapter also showed how to compute the thermal mass for a subsystem delineated by significant variation between the actual and thermal mass. The initial reentry analysis in DAS indicate that 14% of the spacecraft mass will be non-demisable. However further analysis by higher fidelity analysis tools like ORSAT is required to ascertain survivability. Hardware Design-for-Demise methods described in Section 4.3.1 will be employed on parts determined to be non-demisable to make them demisable.

Chapter 6

Conclusion

This thesis examined various aspects involved in designing missions passing through LEO whilst in operation, such that spacecraft completely demise upon uncontrolled reentry into the Earth's atmosphere. We investigated the significance and breadth of Design-for-Demise in LEO missions; strategic approaches in planning demisable missions and proposed a decision making process; demisability analysis, analysis software tools and demisable hardware; and demise design methods among other areas. Here, we outline the areas in which this thesis has made contributions towards the effort of designing demisable LEO missions. Finally, we shall outline areas that require further scrutiny.

6.1 Thesis Contribution

During the course of this investigation, a number of key findings were encountered. They constitute the thesis contribution to the effort geared towards Design-for-Demise of uncontrolled reentry missions passing through LEO. These key findings are summarized below.

1. Approach to DfD mission life-cycle phasal implementation
   In contrast to previous treatment of DfD in NASA missions, we proposed an approach that accommodates DfD practices in the activities of each phase throughout the mission life-cycle. As outlined in Section 2.4, this approach ensures that DfD is continuously accounted for, from Pre-Phase A to Phase F of the mission cycle. An exhaustive consideration of DfD guarantees subjection of the mission to the advantages of demisbale missions.

2. Strategy for DfD execution in mission design and planning
   As shown in Figure 2.5 we outlined the steps on how to execute the intentional redesigning of the spacecraft parts in order to make them demisable. The steps proposed detail strategy to execute the DfD activities in a given mission life-cycle phase. This plan will facilitate continuous thorough engagement of DfD practices in mission development and execution.

3. Generic structural description of reentry analysis tools
   In exploring reentry analysis software tools, this thesis generated a general structural description of reentry analysis software tools. As a result, a fast tracked general understanding of how reentry analysis tools function is facilitated. This general structure is shown in Section 3.1 to exist in the DAS and ORSAT tools.

4. DAS limitations
   DAS as a reentry analysis tool is inherently conservative and possesses a relatively lower fidelity. During the course of this investigation, we were able to add to the documented DAS Reentry Module limitations as outlined in Section 3.1.1. This information facilitates a quick measured appreciation of DAS as a reentry analysis tool and points out areas that can be improved in future.

5. *Critical* parts identification plan
   After decomposing the spacecraft into individual parts via the Subsystems Hierarchical Subdivision approach we suggested in Section 3.2.1, the next step is to identify the non-demisable (critical) parts. We have suggested 2 ways to do this; *a)* carryout a DAS reentry analysis, and *b)* develop a database of perennial known survivors from experience and the documented ground impacting reentry spacecraft parts. The latter provides a reference for choosing the demisable parts.

6. DfD decision making methodology
   This thesis introduced the Analytic Deliberative Process decision making process in Section 4.1 to facilitate the decision to design a spacecraft to demise for an uncontrolled atmospheric reentry post-mission disposal option. As required by this process, we identified the DfD Objectives Hierarchy and Attributes for the ADP procedure. As a final step in the *analysis* phase of the ADP process, we formulated the QPMs and

computed the various levels of consequences. This exercise will facilitate the *deliberative* phase of the ADP decision making procedure.

7. Hardware DfD methods
   In Section 4.3.1, this thesis described the different methods that can be employed in re-designing spacecraft components in order to convert them from being non-demisable to become demisable upon reentry into the Earth's atmosphere. Application of these methods will require a trade-off in cost, performance, mass and reliability among others. However, whether used singly or in combination, the methods have the potential to achieve demisability of spacecraft parts that were initially non-demisable..

8. Demonstration of DfD limitations and trade-offs
   Using the propulsion and power subsystems, we investigated the limitations of designing spacecraft parts to demise and how this affects the mission performance and mass among others. As observed in Section 4.3, for a spacecraft comparable to GPM core spaceraft, the demisable COPV tank exhibited some better characteristics than the monolithic non-demisable titanium tank, such as: higher propellant volume for a given tank mass; ability to demise; higher on orbit ΔV performance and better mass fraction realization for the same tank mass. We also demonstrated how trade-offs are conducted between aluminum cased Li-ion batteries and stainless steel cased NiCd batteries whilst converting a non-demisable power subsystem to a demisable one.

9. Application of reentry demisability analysis and interpretation of DAS result
   In chapter 5, we showed how to carry out reentry analysis on an actual mission case application, HETE-2. This activity detailed selection process of the spacecraft parts likely to survive reentry for further analysis; computation of subsystem thermal mass estimate; and interpretation of the results. The HETE-2 mission was selected for this analysis because information on spacecraft parts was readily available. Even though it is a small spacecraft (124 kg), the demonstrated procedure and techniques for determining demisability can be seamlessly extended to a spacecraft of any given mass. Parts identified as non-demisable at this stage are further subjected to analysis by higher fidelity analysis tools like ORSAT before hardware DfD methods are used to re-design and achieve demisability.

6.2 Areas of Future Work

This effort does not cover all the issues related to DfD, consequently, here we mention some of the areas that necessitate further investigation. The second, *deliberation*, phase of the ADP decision making methodology to facilitate DfD decision making needs to be investigated fully. This effort only addressed the *analysis* phase. The ADP process can not only be used to facilitate the decision to design a mission for demise, but also for the type of post-mission disposal procedure.

Case application on a larger mission like GPM core spacecraft to demonstrate the work advocated by this thesis is an endeavor worth looking into. Moreover, this should not only involve the ADP decision making process, reentry analysis and spacecraft parts re-design, but also the mission reliability, availability, schedule, risk and cost should be calculated. The results should be compared to a similar, traditional, non-demisable controlled reentry mission.

6.3 Final Thoughts

Presently, NASA handles demisability as a means of satisifying the requirement to guarantee ground safety within the framework of orbital debris mitigation. Though this is a very crucial issue, additional merits associated with Design-for-Demise do exist that warrant DfD to be applied in a much broader framework. As mentioned in Section 1.2, DfD relatively simplifies the mission and lowers mission cost and risk. Consequently, DfD should be viewed in this broader context especially for missions passing through LEO whilst in operation. Secondly, though the 0.0001 human casualty risk and demisability are vital in LEO post-mission disposal imposed on NASA sanctioned missions, this practice should be extended to include other non-NASA sanctioned missions like LEO commercial communication satellites, military satellites and launch vehicle upper stages.

Table 6.1: **Appendix A**: HETE-2 Individual Parts Mass.

Part Name	Mass (lbm)	Length - x (in)	Length - y (in)	Length - z (in)
electronics box	26.726			
battery box 1 (+X)	9.606	2.11	11.38	5.5
battery box 2 (-X)	9.562	2.11	11.38	5.5
rf x	10.48			
U channel vhf sc, side 1	0.16492	0.062	1.4	19
U channel vhf sc, side 2	0.16492	0.062	1.4	19
U channel vhf sc, back	0.05916	0.8	0.062	19
gtc con	0.207	1.826	1	2.75
gtc plug	0.207	1.826	1	2.75
gtc bracket top	0.066	1.867	0.55	0.75
gtc bracket bottom	0.066	1.867	0.55	0.75
MSS assembly	0.271	2	2.292	2.8
FSS	0.345	1.9	2.355	2.65
power box	9.661	4.1	14.65	5.152
active hinge +x +y (flat)	0.085	2.088	2.5	0.125
active hinge +x +y (bulk)	0.641	2.27	2.9	1
passive hinge +x -y (flat)	0.07	2.75	2.5	0.125
passive hinge +x -y (bulk)	0.124	1.375	2.5	1
active hinge -x -y (flat)	0.085	2.088	2.5	0.125
active hinge -x -y (bulk)	0.641	2.27	2.9	1
passive hinge -x +y (flat)	0.07	2.75	2.5	0.125
passive hinge -x +y (bulk)	0.124	1.375	2.5	1
active hinge +y-x (flat)	0.085	2.5	2.088	0.125
active hinge +y-x (bulk)	0.641	2.9	2.27	1
passive hinge +y +x (flat)	0.07	2.5	2.75	0.125
passive hinge +y +x (bulk)	0.124	2.5	1.375	1
active hinge -y+x (flat)	0.085	2.5	2.088	0.125
active hinge -y+x (bulk)	0.641	2.9	2.27	1
passive hinge -y -x (flat)	0.07	2.5	2.75	0.125
passive hinge -y -x (bulk)	0.124	2.5	1.375	1
TC driver	1.127	5.088	1.063	6.9
TC driver spacer	0.244	4.1	0.09	6.9
LB3 (SXC)	4.099	14.5	4.191	3.5
LB2 (OPT)	4.062	14.5	4.191	3.5
gamma spacer +Y upper mid	0.017	1.42	0.25	0.87
gamma spacer +Y lower mid	0.017	1.42	0.25	0.87
gamma spacer +Y +x upper	0.011	0.83	0.25	0.87
gamma spacer +Y +x lower	0.011	0.83	0.25	0.87
gamma spacer +Y -x upper	0.011	0.83	0.25	0.87
gamma spacer +y -x lower	0.011	0.83	0.25	0.87
gamma spacer -Y upper mid	0.017	1.42	0.25	0.87
gamma spacer -Y lower mid	0.017	1.42	0.25	0.87
gamma spacer -Y +x upper	0.011	0.83	0.25	0.87
gamma spacer -Y +x lower	0.011	0.83	0.25	0.87
gamma spacer -Y -x upper	0.011	0.83	0.25	0.87
gamma spacer -y -x lower	0.011	0.83	0.25	0.87
OSC +x	0.76927617	0.15	7.586	6.143

Part Name	Mass (lbm)	Length - x (in)	Length - y (in)	Length - z (in)
OSC +y	1.62099335	15.85	0.17	6.143
OSC -y	1.62099335	15.85	0.17	6.143
SS +x	1.13572383	0.17	7.746	7.14
SS-x	1.15381783	0.17	7.746	7.14
SS +y	2.26200665	16.325	0.17	7.102
SS -y	2.28400665	16.325	0.17	7.102
SS mid rib	1.516	0.2	7.694	6.7
WXM coded mask	0.323	16.8	8.2	0.02
WXM code mask ring	0.3886	16.8	8.2	0.25
WXM	21.716	14.961	7.441	6.654
Fregate electronics	9.9	5.118	11.811	4.685
mo wheel spacer top+	0.5092	3.3	0.45	3.3
MW spacer wall (+Z)	0.185	3.7	2.5	0.2
MW spacer wall (-Z)	0.185	3.7	2.5	0.2
MW spacer wall (+X)	0.185	0.2	2.5	3.7
MW spacer wall (-X)	0.185	0.2	2.5	3.7
MW spacer flange (+Z)	0.0447	3.7	0.2	0.55
MW spacer flange (-Z)	0.0447	3.7	0.2	0.55
MW spacer flange (+X)	0.0447	0.55	0.2	3.7
MW spacer flange (-X)	0.0447	0.55	0.2	3.7
mo wheel driver	0.775	3.439	1.062	6.976
SAX	1.395	0.9	9.58	4.4
interface plate	14.202	17.8	17.8	0.6
panel restraint +x box	0.24	1.65	1.9	2.1
panel restraint -x box	0.24	1.65	1.9	2.1
panel restraint +y box	0.226	1.9	1.65	2.1
panel restraint -y box	0.226	1.9	1.65	2.1
snubber +x +y	0.091	1.8	0.75	0.75
snubber +x -y	0.091	1.8	0.75	0.75
snubber -x +y	0.091	1.8	0.75	0.75
snubber -x +y	0.091	1.8	0.75	0.75
snubber +y +x	0.091	0.75	1.8	0.75
snubber +y -x	0.091	0.75	1.8	0.75
snubber -y+x	0.091	0.75	1.8	0.75
snubber -y-x	0.091	0.75	1.8	0.75
snubber bracket +x +y	0.081	0.266	2.75	1.15
snubber bracket+x -y	0.081	0.266	2.75	1.15
snubber bracket -x +y	0.081	0.266	2.75	1.15
snubber bracket-x -y	0.081	0.266	2.75	1.15
snubber bracket +y +x	0.304	1.15	4.538	1.15
snubber bracket+y -x	0.304	1.15	4.538	1.15
snubber bracket-y+x	0.304	1.15	4.538	1.15
snubber bracket-y-x	0.304	1.15	4.538	1.15
pickup block -Z, +x+y	0.151	1.5	1	1.022
pickup block -Z, +x-y	0.151	1.5	1	1.022
pickup block -Z, -x+y	0.151	1.5	1	1.022
pickup block -Z, -x-y	0.151	1.5	1	1.022

Part Name	Mass (lbm)	Length - x (in)	Length - y (in)	Length - z (in)
WXM cal source 1	0.095	0.9	0.5	1.5
WXM cal source 2	0.095	0.9	0.5	1.5
WXM cal source 3	0.095	0.9	0.5	1.5
WXM cal source 4	0.095	0.9	0.5	1.5
WXM cal source 5	0.095	0.5	0.9	1.5
WXM cal source 6	0.095	0.5	0.9	1.5
WXM cal source 7	0.095	0.5	0.9	1.5
WXM cal source 8	0.095	0.5	0.9	1.5
patch antenna +Z	0.893	4.95	8.45	0.25
magnetometer sc	0.33	1.28	1.41	4.03
mag sc bracket part 1	0.068	0.05	1.41	5.65
mag sc bracket part 2	0.018	1.2	0.1	1.5
mag ss spacer	0.22	0.452	1.41	5.65
gps	2.235	3.976	5.984	2.205
z tc spacer +x	0.072	0.9	4.8	0.18
z tc spacer -x	0.072	0.9	4.8	0.18
z tc spacer +y	0.072	4.8	0.9	0.18
z tc spacer -y	0.072	4.8	0.9	0.18
battery box 3	9.17	2.11	11.38	5.34
battery box 3 +Z lid	0.501	2.12	11.38	0.18
battery box 3 -Z lid	0.61	2.527	11.38	0.18
SP +X-Y bracket, p1	0.02144	1.2	0.062	3.8
SP +X-Y bracket, p2	0.02356	0.062	1	3.8
SP +X+Y bracket, p1	0.01674	1.2	0.062	2.3
SP +X+Y bracket, p2	0.01426	0.062	1	2.3
SP -X+Y bracket, p1	0.02344	1.2	0.062	3.8
SP -X+Y bracket, p2	0.02356	0.062	1	3.8
battery power bracket w/ D9x3-D25)	0.18	1.2	1.5	4.2
css +z +x +y & bracket	0.053	1.375	1	1.375
css +z +x -y & bracket	0.053	1.375	1	1.375
digital watch	0.511	4.924	0.712	3.774
aux buffer (TCD)	0.18	2.38	0.641	2.25
aux buffer (MWD)	0.18	2.38	0.641	2.25
aux buffer (DW)	0.18	2.25	0.641	2.38
aux buffer (aux buffer)	0.18	2.25	0.641	2.38
RF test bracket	0.042	3.73	1.09	0.9
TB, Fregate +Y +x	0.038795849	0.125	4	7.75
TB, Fregate +Y +y	0.073408303	7.75	0.125	7.75
TB, Fregate +Y -x	0.038795849	0.125	4	7.75
TB, Fregate -Y +x	0.038795849	0.125	4	7.75
TB, Fregate -Y -y	0.073408303	7.75	0.125	7.75
TB, Fregate -Y -x	0.038795849	0.125	4	7.75
TB, +X	0.045	0.125	12	4.5
TB, +Y	0.2	18	0.125	14
TB, -X	0.12	0.125	17	5.75
TB, -Y	0.15	17.5	0.125	7
ACS bracket +X	0.209	2.9	3.48	2.47

Part Name	Mass (lbm)	Length - x (in)	Length - y (in)	Length - z (in)
ACS sunshield +X	0.216	7.07	4.49	0.062
ACS sunshield -X	0.216	7.07	4.49	0.062
makeFlat spacer -Y+x	0.014	3.58	0.062	2.92
makeFlat spacer -Y-x	0.014	3.58	0.062	2.92
makeFlat spacer +Y+x	0.014	3.58	0.062	2.92
makeFlat spacer +Y-x	0.014	3.58	0.062	2.92
makeFlat -X	0.106	3.578	0.184	3
makeFlat +X	0.106	3.578	0.184	3
SXC truss base -X	0.122	3.578	0.15	3
SXC truss base +X	0.122	3.578	0.15	3
SXC truss 1 (-X)	0.328	0.25	8.2	3
SXC truss 2-	0.249	0.25	4.19	3
SXC truss 3 (-X)	0.073	0.25	3.265	3
SXC truss 1 (+X)	0.328	0.25	8.2	3
SXC truss 2+	0.249	0.25	4.19	3
SXC truss 3 (+X)	0.073	0.25	3.265	3
SXC truss bottom +X	0.314	8	8	0.05
SXC truss bottom -X	0.314	8	8	0.05
SXC baseplate -X	0.836	9	9	0.25
SXC baseplate +X	0.84	9	9	0.25
SXC box -X 1	0.465	0.2	4.5	4.587
SXC box -X 2	0.465	4.5	0.2	4.587
SXC box -X 3	0.465	0.2	4.5	4.587
SXC box -X 4	0.465	4.5	0.2	4.587
SXC box +X 1	0.465	0.2	4.5	4.587
SXC box +X 1	0.465	4.5	0.2	4.587
SXC box +X 1	0.465	0.2	4.5	4.587
SXC box +X 1	0.465	4.5	0.2	4.587
SXC missing mass +X	-0.106	4.5	4.5	4.59
SXC missing mass -X	-0.106	4.5	4.5	4.59
ACS OPT missing mass -X	0.059	4.5	4.5	4.59
ACS OPT missing mass +X	0.065	4.5	4.5	4.59
SXC +X radiator 1	0.111	0.05	2.425	7.5
SXC +X radiator 2	0.156	0.05	3.43	7.5
SXC +X radiator 3	0.076	0.05	1.66	7.5
SXC +X radiator 4	0.137	0.05	3.02	7.5
SXC +X rad bracket outer	0.42	1.5	0.04	7.5
SXC +X rad bracket inner	0.51	0.04	2.1	7.5
SXC -X radiator 1	0.111	0.05	2.425	7.5
SXC -X radiator 2	0.156	0.05	3.43	7.5
SXC -X radiator 3	0.076	0.05	1.66	7.5
SXC -X radiator 4	0.137	0.05	3.02	7.5
SXC -X rad bracket outer	0.42	1.5	0.04	7.5
SXC -X rad bracket inner	0.51	0.04	2.1	7.5

Part Name	Mass (lbm)	Diameter (in)	Length - z (in)	Diameter -inner(in)
marman ring, bolt flange	0.579844738	17.75	0.125	16
marman ring, sidewall	0.606955701	16.2	1.2	16
marman ring, top flange	1.613199562	16.6	0.15	14.2
Z TC sunshield	0.236	12.5	0.05	10.5
TC x	5.544	6.2	1.6	3.62
TC y	3.552	9.1	0.902	7.234
TC z	3.523	12.45	1.172	11.5
panel restraint +x cyl	0.0926	0.52	1.897	
panel restraint -x cyl	0.0926	0.52	1.897	
panel restraint +y cyl	0.0926	0.52	1.897	
panel restraint -y cyl	0.0926	0.52	1.897	
Bsite camera 1 (+y+x)	1.36	2.8875	5.538	
Bsite camera 2(+y-x)	1.364	2.8875	5.538	
Bsite camera mnshld1 (+y+x)	0.04	2.24	1.5	2.16
Bsite camera mnshld2(+y-x)	0.04	2.24	1.5	2.16
Bsite camera filter (+y+x)	0.031	2	0.125	
Bsite camera filter(+y-x)	0.031	2	0.125	
ACS camera 2 (-y-x)	1.936	4	5.406	
ACS camera 1 (-y+x)	1.947	4	5.406	
ACS moonshield 1 (-y-x)	0.11	3.25	2.875	3.125
ACS moonshield 2 (-y+x)	0.11	3.25	2.875	3.125
Fregate 1	4.813	3.78	8.04	
Fregate 2	4.813	3.78	8.04	
Fregate 3	4.748	3.78	8.04	
Fregate 4	4.748	3.78	8.04	
Z antenna standoff 1	0.04	0.268	2.716	
Z antenna standoff 2	0.04	0.268	2.716	
Z antenna standoff 3	0.04	0.268	2.716	
Z antenna standoff 4	0.04	0.268	2.716	
Z TC sunshield standoff 1	0.018	0.268	1.25	
Z TC sunshield standoff 2	0.018	0.268	1.25	
Z TC sunshield standoff 3	0.018	0.268	1.25	
Z TC sunshield standoff 4	0.018	0.268	1.25	
Z TC sunshield standoff 5	0.018	0.268	1.25	
Z TC sunshield standoff 6	0.018	0.268	1.25	
Z TC sunshield standoff 7	0.018	0.268	1.25	
Z TC sunshield standoff 8	0.018	0.268	1.25	
SXC +X shield standoff	0.04	0.268	3	
SXC +X shield standoff	0.04	0.268	3	
SXC +X shield standoff	0.04	0.268	3	
SXC -X shield standoff	0.04	0.268	3	
SXC -X shield standoff	0.04	0.268	3	
SXC -X shield standoff	0.04	0.268	3	
gps antenna	0.249	3.78	0.153	
gps antenna mount	0.483	2.953	2.8	
moment wheel and blanket	5.334	10.04	2.148	
CSS +X-Z	0.02	0.5	0.354	
CSS -X-Z	0.02	0.5	0.354	
harness	10.65520387			

Bibliography

[1] National Aeronautics and Space Administration, Washington, DC 20546, USA, *NASA TECHNICAL STANDARD - Process for Limiting Orbital Debris*, NASA-STD-8719.14 ed., August 2007. Expiration Date: 28 August 2012.

[2] U. S. Government, *United States Government Orbital Debris Mitigation Standard Practices*, 1997.

[3] NASA Goddard Spaceflight Center [Online Source], *Compton Gamma Ray Observatory Mission Website*. [cited 2008 July 14], Available HTTP: http://cossc.gsfc.nasa.gov/docs/cgro/.

[4] NASA Goddard Spaceflight Center [Online Source], *Gamma-ray Large Area Space Telescope Mission Website*. [cited 2008 July 14], Available HTTP: http://glast.gsfc.nasa.gov/.

[5] J. Leibee, T. Ford, and A. Whipple, "NASA GLAST Project Experiences Managing Risks of Orbital Debris," in *Eigth International Conference on Space Operations*, (Montreal, Canada), American Institute of Aeronautics and Astronautics, May 17-21 2004.

[6] NASA Goddard Spaceflight Center [Online Source], *Global Precipitation Measurement Mission Website*. [cited 2008 July 15], Available HTTP: http://gpm.gsfc.nasa.gov/.

[7] W. Rochelle, and R. Kinsey, and E. Reid, and R. Reynolds, and N. Johnson, "Spacecraft orbital debris reentry aerothermal analysis," in *IADC Meeting*, (Houston, TX), Inter-Agency Space Debris Coordination Committee, December 1997.

[8] NASA Astromaterials Research and Exploration Science Directorate. Orbital Debris Program Office, Lyndon B. Johnson Space Center, Houston, Texas, *Debris Assessment Software User's Guide. Version 2.0*, November 2007.

[9] M. D. Griffin and J. R. French, *Space Vehicle Design*. AIAA Education Series, Reston, VA: American Institute of Aeronautics and Astronautics, Inc., 2^{nd} ed., 2004.

[10] S. A. Bouslog, B. P. Ross, and C. B. Madden, "Space Debris Reentry Risk Analysis," in *32nd Aerospace Sciences Meeting and Exhibit*, (Reno, NV), American Institute of Aeronautics and Astronautics, January 10-13, 1994.

[11] National Aeronautics and Space Administration, Washington, DC 20546, USA, *NASA Safety Standard - Guidelines and Assessment Procedures for Limiting Orbital Debris*, NSS1740.14 ed., August 1995.

[12] W. L. Hankey, *Re-Entry Aerodynamics*. AIAA Education Series, Washington, DC: American Institute of Aeronautics and Astronautics, Inc., 1988.

[13] National Aeronautics and Space Administration, Washington, DC 20546, USA, *NASA Procedural Requirements for Limiting Orbital Debris*, NPR 8715.6A ed., February 2008. Expiration Date: 19 Februaury 2013.

[14] National Aeronautics and Space Administration, Washington, D.C., USA, *NASA Systems Engineering Handbook*, NASA/SP-2007-6105 Rev1 ed., December 2007.

[15] T. Lips and B. Fritsche, "A comparison of commonly used re-entry analysis tools," *Acta Astronautica*, vol. 57, pp. 312–323, July 2005.

[16] H. Klinkrad, T. Lips, and B. Fritsche, "A Standardized Method For Re-Entry Risk Evaluation," in *55th International Astronautical Congress of the International Astronautical Federation, the International Academy of Astronautics, and the International Institute of Space Law*, (Vancouver, Canada), American Institute of Aeronautics and Astronautics, 2004.

[17] J. Dobarco-Otero, R. N. Smith, K. J. Bledsoe, R. M. DeLaune, W. C. Rochelle, and N. L. Johnson, "The Object Reentry Survival Analysis Tool (ORSAT)-Version 6.0 and its Application to Spacecraft Entry," in *56th International Astronautical Congress of*

the International Astronautical Federation, the International Academy of Astronautics, and the International Institute of Space Law, (Fukuoka, Japan), American Institute of Aeronautics and Astronautics, October 17-21, 2005.

[18] J. Dobarco-Otero, R. N. Smith, J. J. Marichalar, J. N. Opiela, W. C. Rochelle, and N. L. Johnson, "Upgrades to Object Reentry Survival Analysis Tool (ORSAT) for Spacecraft and Launch Vehicle Upper Stage Applications," in *54th International Astronautical Congress of the International Astronautical Federation, the International Academy of Astronautics, and the International Institute of Space Law*, (Bremen, Germany), American Institute of Aeronautics and Astronautics, September 29 - October 3, 2003.

[19] J. Opiela and N. Johnson, "Improvements to NASA's Debris Assessment Software," in *58th International Astronautical Congress of the International Astronautical Federation, the International Academy of Astronautics, and the International Institute of Space Law*, (Hyderabad, India), American Institute of Aeronautics and Astronautics, September 24 - 29, 2007.

[20] T. Lips and B. Fritsche, "A Comparison of Commonly Used Reentry Analysis Tools," in *International Academy of Space Debris and Space Traffic Managements Symposium held in conjuction with 55th International stronautical Congress*, (Vancouver, Canada), American Astronautical Society, October 4-8, 2004.

[21] B. Fritsche, T. Lips, and G. Koppenwallner, "Analytical and Numerical Reentry Analysis of Simple Shaped Objects," in *54th International Astronautical Congress of the International Astronautical Federation, the International Academy of Astronautics, and the International Institute of Space Law*, (Bremen, Germany), American Institute of Aeronautics and Astronautics, September 29 - October 3, 2003.

[22] A. J. Eggers and H. J. Allen, "A study of the motion and aerodynamic heating of missiles entering the earth's atmosphere at high supersonic speeds," in *TN-4047*, (Washington), National Advisory Committee for Aeronautics, 1957.

[23] X. N. Vinh, *Hypersonic and Planetary Entry Flight Mechanics*. Ann Arbor, MI: University of Michigan Press, June 1980.

[24] S. F. Hoerner, *Fluid Dynamic Drag*. Published by Author, 1965.

[25] R. W. Detra, N. H. Kemp, and F. R. Riddell, "Heat Transfer to Satellite Vehicles Reentering the Atmosphere (addendum)," *Jet Propulsion*, vol. 27, pp. 1256–1257, December 1957.

[26] J. N. Opiela and M. J. Matney, "Improvements to NASA's Estimation of Ground Casualties from Reentring Space Objects," in *54th International Astronautical Congress of the International Astronautical Federation, the International Academy of Astronautics, and the International Institute of Space Law*, (Bremen, Germany), American Institute of Aeronautics and Astronautics, September 29 - October 3, 2003.

[27] NASA Orbital Debris Program Office [Online Source], *Debris Assessment Softaware (DAS) 2.0.1 Website*. [cited 2008 April 23], Available HTTP: http://orbitaldebris.jsc.nasa.gov/mitigate/das.html.

[28] T. Lips, B. Fritsche, G. Koppenwallner, A. Zaglauer, and R. Wolters, "Reentry Analysis of TERRASAR-X with SCARAB," in *54th International Astronautical Congress of the International Astronautical Federation, the International Academy of Astronautics, and the International Institute of Space Law*, (Bremen, Germany), American Institute of Aeronautics and Astronautics, September 29 - October 3, 2003.

[29] W. J. Larson and J. R. Wertz, eds., *Space Missions Analysis and Design*. Space Technology Series, El Segundo, CA: Microcosm Press, 3^{rd} ed., 2006.

[30] V. L. Pisacane and R. C. Moore, eds., *Fundamentals of Space Systems*. JHU/APL Series in Science and Engineering, New York, NY: Oxford University Press, 2^{nd} ed., 2005.

[31] H. Klinkrad, *Space Debris Models and Risk Analysis*. Chichester, UK: Praxis Publishing Ltd, 2006.

[32] L. Pagani, C. Smith, and G. Apostolakis, "Making Decisions for Incident Management in Nuclear Power Plants Using Probabilistic Safety Assessment," *Risk, Decision and Policy*, pp. 271–295, September 2004.

[33] M. Stamatelatos, H. Dezfuli, and G. Apostolakis, "A Proposed Risk- Informed Decision-Making Framework for NASA," in *8th International Conference on Probabilistic Safety Assessment and Management*, (New Orleans, Louisiana), International Association of Probabilistic Safety Assessment and Management, May 15-18, 2006.

[34] J. C. Mankins, *Technology Readiness Levels - A White Paper*. NASA, Advanced Concepts Office, Office of Space Access and Technology, April 6, 1995.

[35] ANSI/AIAA S-081A-2006 Standard, Reston VA, *Space Systems - Composite Overwrapped Pressure Vessels*, December 2006.

[36] NASA Goddard Spaceflight Center [Online Source], *Demiseable Reaction Wheel Assembly Website*. [cited 2008 November 12], Available HTTP:
http://ipp.gsfc.nasa.gov/ft-tech-demis-react-whl.html.

[37] Massachusetts Institute of Technology, Kavli Institute for Astrophysics and Space Research (MKI) [Online Source], *High Energy Transient Explorer Mission Website*. [cited 2008 November 3], Available HTTP:
http://space.mit.edu/HETE/.

Index